Received November 4, 2019, accepted November 25, 2019, date of publication December 2, 2019,
date of current version December 23, 2019.

*Digital Object Identifier 10.1109/ACCESS.2019.2957062*

# Wind Speed Forecasting System Based on the Variational Mode Decomposition Strategy and Immune Selection Multi-Objective Dragonfly Optimization Algorithm

**HE BO [1], XINSONG NIU [2], AND JIANZHOU WANG [2]**

[1]Dongbei University of Finance and Economics Postdoctoral Research Mobile Station, Dalian 116025, China
[2]School of Statistics, Dongbei University of Finance and Economics, Dalian 116025, China

Corresponding author: Xinsong Niu (xinsongniu@gmail.com)

This work was supported by the National Natural Science Foundation of China under Grant 71671029.

**ABSTRACT** In the development of the wind power industry, short-term wind speed forecasting is necessary, and many researchers have made substantial efforts to establish wind speed prediction models. However, realizing the accurate prediction of wind speeds remains a challenging task. The current prediction models do not consider the preprocessing of the data, and each model has various shortcomings. Considering the disadvantages of the available models, in this paper, an advanced combined forecasting system is applied that utilizes a data preprocessing strategy and parameter optimization strategy to obtain accurate prediction values. The proposed prediction system employs linear and nonlinear models that can take into account the characteristics of wind speed sequences, successfully combine the advantages of various single models, and yield accurate and stable prediction values. Finally, according to the experimental analysis and discussion, the proposed combined prediction system outperforms the compared models in prediction. In conclusion, the powerful combined prediction model provides a feasible scheme for wind power prediction.

**INDEX TERMS** Artificial intelligence, combined forecasting system, data preprocessing, developed optimization algorithm, wind speed forecasting.

## I. INTRODUCTION

Resource depletion and global climate change are becoming increasingly severe. Accelerating the extraction and utilization of clean energy is an effective approach for solving these problems. In recent years, the use of renewable energy power generation technology has become increasingly widespread. Compared with traditional power generation methods, renewable energy power generation technology has many advantages [1]. Renewable energy not only protects the natural environment but also makes more effective use of limited space. Wind energy, as an environmentally friendly energy source, is an important type of renewable resource and occupies a dominant position in the world's energy mix [2].

Wind energy is the energy that is produced by the movement of air on the surface of the earth. It is favored by many countries because it is regenerative and clean [3]. Coastal and open continental contraction belts are rich in wind energy resources. From the perspective of regional distribution, North America, Asia and Latin America are major sources of wind energy resources. According to estimates by authoritative institutions, the total amount of wind power in the world is approximately 130 billion kilowatts, and the portion that can be used is approximately 15%, which is 10 times that of hydropower resources, and can reach 53 trillion kilowatt hours per year. China is very rich in wind power resources. Vigorously developing the wind power industry is regarded as an important measure for transforming the development model and realizing sustainable development. According to statistics from the Global Wind Energy Council (GWEC), from the perspective of the development of the entire global wind power industry, the total installed capacity has been increasing year by year. In 2017, the cumulative installed capacity of global wind power was approximately 539 GW [4]. **Fig. 1** presents the regions of the world with high installed wind power capacity.

The associate editor coordinating the review of this manuscript and approving it for publication was Taufik Abrao.

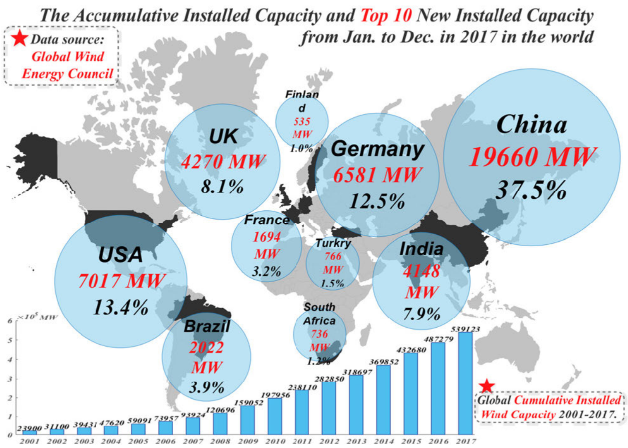


**FIGURE 1.** Application of wind energy resources on the global scale.

In the past decade, due to the strong support of the Chinese government, wind energy has played an indispensable role in China's energy industry structure. In addition, due to the large amount of power resources provided by the wind power industry, the recent power shortages in China were effectively alleviated [5]. The prediction and assessment of wind energy resources are practical and challenging tasks [6].

Over the years, many methods have been proposed for the prediction of wind energy, and these prediction methods are divided into the following categories: physical methods, general statistical methods, artificial intelligence methods, and combined models (or hybrid models) [7], [8]. Numerical weather prediction (NWP) modeling is a typical method that uses physical models, and these physical models have great advantages in the field of long-term prediction [9]. However, the physical models require substantial support from meteorological data, which complicates the prediction [10]. The general statistical modeling methods mainly include the autoregressive (AR) method, the autoregressive moving average (ARMA) method, and the autoregressive integrated moving average (ARIMA) method. These linear models show good performance in short-term predictions [11], [12]. However, the nonlinear characteristics of time series render accurate prediction impossible [13].

In the past years, artificial intelligence (AI) methods have developed rapidly and have been applied to a variety of fields. Many researchers have used these approaches to prediction, especially in the field of wind energy forecasting. Artificial neural networks (ANNs) such as the echo state network (ESN), extreme learning machine (ELM), and the back-propagation neural network (BPNN) are typical AI methods [14]–[17]. Other AI approaches include support vector machine (SVM) and least-squares support vector machine (LSSVM) [18]. Intelligent methods have been widely used in economic forecasting, energy forecasting, power load forecasting, and even air quality predictions [19]–[22]. Among them, the ANN method can accurately capture the nonlinear features in the time series. If the sequence has strong nonlinear features, it shows good prediction performance on the prediction surface, and can realize high prediction accuracy. According to Ma et al, the ANN method can describe the complex relationships in historical data; hence, it is a suitable method for predicting wind speed [23]. For example, Li & Shi considered the wind speed sequence in hours as a comparison experiment, and via the comparative analysis of various neural network methods, they found that each single method has its own advantages and disadvantages [24]. Wang et al. applied a method that uses ESN, compared it with other ANNs methods, and obtained more accurate prediction results [25]. In addition, Niu et al. demonstrated that the ANNs approach has the natural advantage of being able to extract the nonlinear features of the sequence and, hence, realizes more accurate predictions than other methods [26]. In recent years, deep learning applications have grown rapidly due to the satisfactory performance of deep learning in dealing with big data and high-performance computing power. Wang et al. proposed deep convolutional neural network (DCNN) based wavelet transform (WT) for forecasting photovoltaic (PV) energy and obtained accurate results [27]. Hu et al. used the long short-term memory neural network (LSTM), the hysteretic extreme learning machine (HELM) and the differential evolution algorithm (DE) methods to forecast wind energy data and obtained a satisfactory forecasting result [28].

Each forecasting model has disadvantages, and no prediction model is perfect [29], [30]. Hence, researchers have recently shifted their attention to combined and hybrid models, which can produce more accurate predictions by combining several approaches. For instance, Hao & Tian proposed an improved nonlinear combined prediction system, which processed the original data via a data preprocessing approach and used a developed SVM to combine all single predictors to obtain the final forecasting results. This approach overcame the shortcomings of the single models and yielded accurate prediction results [31]. Ma & Liu applied the kernel function method to the grey model, proposed a new time-series forecasting model, and demonstrated that this method outperforms the traditional grey model in practical applications [32]. Heng et al. proposed a hybrid prediction model that is based on empirical mode decomposition (EMD) and the cuckoo search algorithm, which is used to obtain more accurate results for power load forecasting [33]. Wang et al. proposed another hybrid prediction method for wind speed prediction that uses the decomposition method, BPNN and the genetic algorithm (GA) [34]. In addition, Zhou et al. proposed a new approach that combines multiple single prediction models via the genetic algorithm and particle swarm optimization to obtain a combined prediction model, and they demonstrated that developed model has superior prediction performance [35]. Several additional examples are listed in **Table 1**.

Previous traditional models have flaws that can lead to inaccurate predictions. The combined (hybrid) model is superior to single traditional models, but most combined (hybrid) models focus on the improvement of the model forecasting

**TABLE 1.** Summary of reviewed wind speed forecasting models.

| Model | dataset | Result | Advantage | Disadvantage |
|---|---|---|---|---|
| **Physical forecasting method** | | | | |
| NWP methods [36] | Wind energy data in Malaysia | Through economic analysis, the researchers found that Malaysia has high wind energy potential, in contrast to widespread publicity. | Has great advantages in the field of long-term forecasting and plays an important role in long-term forecasting. | The physical model requires substantial support from meteorological data, which renders the prediction more complicated and provides only ultra-short-term wind speed forecasting. |
| Spatial correlation method [37] | Wind direction with wind speed | Wind image data are used to improve the prediction accuracy of the wind speed. | | |
| Numerical weather prediction Eta model [38] | Wind energy data collected from the Nasudden power plants | The Eta model is applicable as a meteorological driver for wind energy modeling and prediction. | | |
| etc. | | | | |
| **Statistical forecasting methods** | | | | |
| Hammerstein model , AR method [39] | Three years (2004–2006) from two different sites | The HAR model is suitable for a short term 1–24 h forecast horizon. | For short-term wind speed prediction, the statistical model has more advantages and has higher potential for short-term forecasting. | These models are linear and they do not effectively capture the nonlinear characteristics of the data sequence. |
| ARIMA [40] | Historical and synthetic wind speed data | The accuracy of the ARIMA for the first 6–8 hours of wind speed prediction is lower when it is used for longer periods of time. | | |
| Fractional-ARIMA [41] | Hourly average wind speeds from North Dakota | This model can improve the accuracy of wind energy forecasting when compared to the persistence method. | | |
| etc. | | | | |
| **Artificial intelligent forecasting technologies** | | | | |
| ANNs [42] | 24 hourly mean wind speed data from La Venta, Oaxaca., México | The developed model for short term wind speed forecasting showed a very good accuracy | They can identify nonlinear relationships in the dataset regardless of whether the relationships are known or not. | The drawbacks of ANN models include becoming trapped by local minima, overfitting problems, being limited by insufficient data and requiring larger samples. |
| Differential polynomial neural networks [43] | Hourly data for a period of 1–3 days | The proposed model is a new neural network type, which can model more complex dynamic processes. | | |
| LSSVM [44] | Hourly wind speed from North Dakota, USA. | LSSVM outperforms the persistence model in most of cases. | | |
| etc. | | | | |
| **Combined/Hybrid forecasting technologies** | | | | |
| EMD and ELM[45] | Xinjiang wind farm in China | The proposed hybrid models show higher forecasting accuracy than the ARIMA and the persistence model, among others. | By integrating the individually superior features of multifarious algorithms/models, they can realize higher prediction accuracy than other models. | Each hybrid model is designed by researchers according to their considerations and shows highly promising results on a set of practical problems under limited conditions but may perform poorly on other problems. |
| SSA, PSO and BPNN [46] | Wind speed data collected from Penglai in China | The proposed method can improve the forecasting accuracy and is suitable for short-term wind speed forecasting. | | |
| Adaptive boosting strategy[18] | Short-term wind speed data collected from China | This hybrid model is more efficient and can yield more accurate wind speed forecasts than the benchmark models from the literature. | | |
| etc. | | | | |
| **Deep learning technologies** | | | | |
| WT and DCNN [27] | Datasets from a northwestern Flanders PV farm and a northeastern Limburg PV farm | The proposed methods increased forecasting accuracies under seasonal variations and various prediction horizons. | Its capability for dealing with big data and high-performance computing power. | The representation performance of deep learning does not mean that deep learning performs better for learning nonlinear functions, and it is theoretically difficult for deep learning to train the deep network and to optimize its parameters [47]. |
| Grey theory and deep belief network [48] | Five-MW PV power plant in central Taiwan | The proposed GT-DBN model outperforms other models in terms of forecasting accuracy and is suitable for day-ahead PV power output prediction. | | |
| Stacked autoencoder Levenberg–Marquardt [49] | Real-world data collected from the M6 freeway in the U.K. | The deep architecture of the neural network approach is used to realize accurate traffic forecasting. | | |
| etc. | | | | |

accuracy and often ignore the importance of predictive stability. The forecasting accuracy and stability of the model must be guaranteed, and both need to be considered comprehensively. Therefore, the single-objective optimization method cannot solve this problem, and a multi-objective optimization method needs to be considered.

For the above discussion, a developed combined wind speed prediction system that is based on the variational mode decomposition (VMD) approach and the immune selection multi-objective dragonfly optimization algorithm (ISMODA) is applied for multi-step wind speed prediction. The proposed combined wind speed prediction system consists of four main parts: the data preprocessing part, the optimization part, the prediction part and the evaluation part. This combined wind speed forecasting system overcomes the shortcomings of single-model prediction and can capture the nonlinear features of the wind energy sequence accurately, which not only greatly improves the accuracy but also ensures the stability of the prediction. In the data preprocessing stage, the wind energy data are decomposed via a decomposition strategy to eliminate the high-frequency noise signals. Moreover, in the forecasting stage, four single forecasting components are used for short-time wind speed prediction, namely, three ANN models and a linear model. Next, an advanced multi-objective optimization algorithm, namely, ISMODA, is used to determine the weights of the four single-model components and to obtain the final combined model results. To the best of our knowledge, determining the weight of a single model via this method can combine the advantages of each component well and can yield highly accurate wind speed forecasting results.

**The forward-looking contributions and innovations of this paper are as follow:**

**I.** The stability and accuracy of the prediction are taken into account. In the prediction of wind speed series, stability is an important index, but it is easy to ignore. Therefore, a multi-objective optimization method is used to improve the accuracy and stability of the system.

**II.** An improved optimization algorithm that uses the immune selection operator is applied to the construction of prediction system. The improved algorithm can update the population using immune selection operations in the late optimization iteration. Via this approach, it can effectively suppress the premature stagnation problem in the convergence process and improve its global optimization performance and optimization accuracy.

**III.** The organic combination of linear and nonlinear models has strong linear and nonlinear characteristics. The proposed combined prediction system combines the advantages of each model, captures the linear and nonlinear characteristics of the data series, and yields stable and accurate prediction results.

The structure of this paper is as below. Theoretical introduction of VMD and ISMODA algorithm are shown in Section 2. The information of the data is summarized in Section 3. In Section 4, we introduce the accuracy evaluation index and validity evaluation index in detail. Several comparative experiment analyses are displayed in Section 5. Section 6 draws several discussions to confirm the forecasting models. Finally, the summary is placed in Section 7. The main flow of the article is shown in **Fig. 2**.

## II. METHODS INTRODUCTION

In this section, the methods that are proposed in the paper are discussed in detail. These are VMD data preprocessing method and the immune selection multi-objective optimization dragonfly algorithm (ISMODA).

### A. VARIATIONAL MODE DECOMPOSITION

VMD is an effective technique for preprocessing signals that outperforms other signal processing approaches. The VMD method is based on variational constraint theory and can decompose real-valued signals into modalities with nonrecursive screening structures [50]. Each decomposition mode

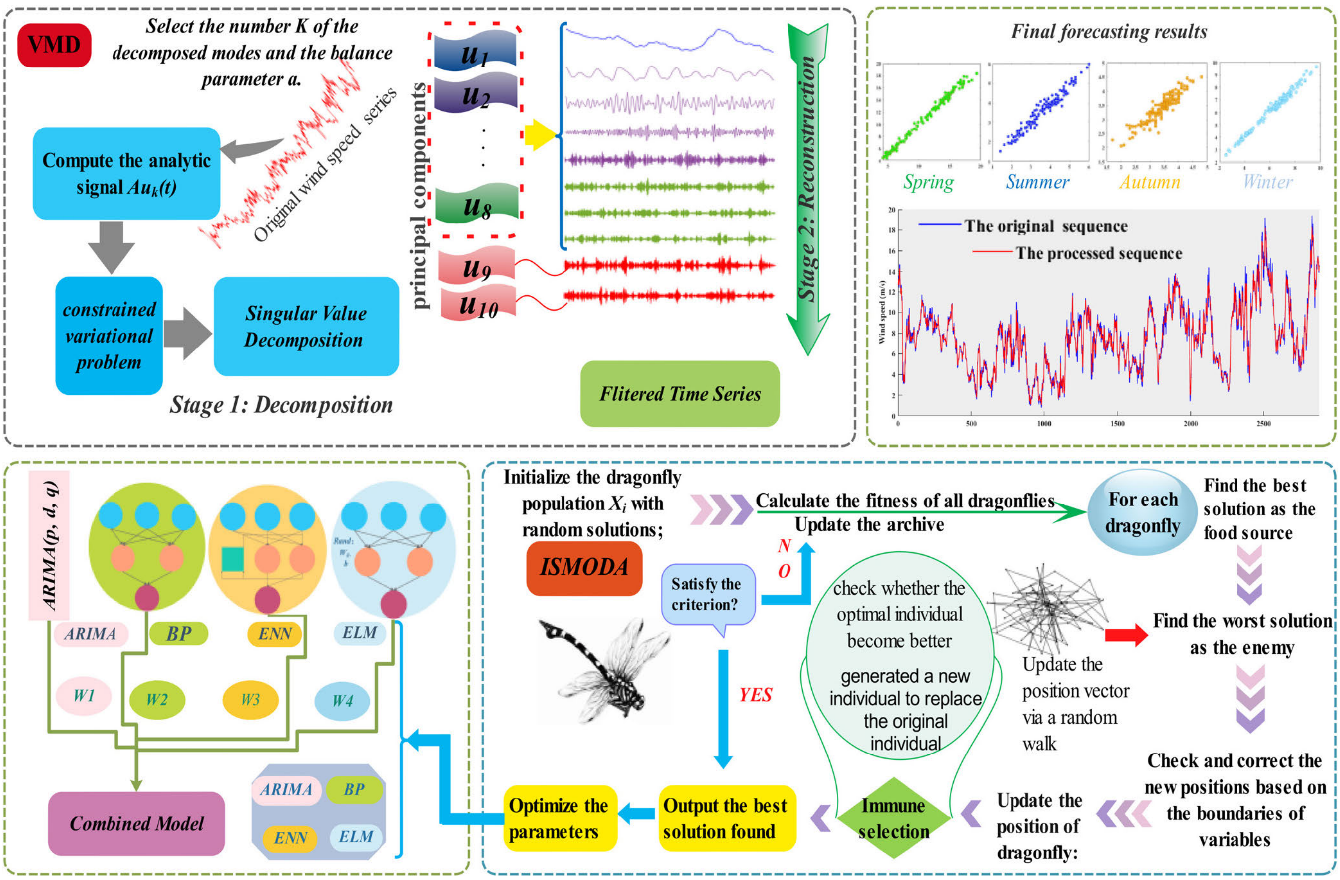


**FIGURE 2.** Main structure of this study.

is a quasi-orthogonal band-limited subsignal that is sparse and must be the most compact near its center frequency. The implementation process of the VMD method is as follows:

*Step 1:* Determine the number of decomposition modes $\boldsymbol{u_k}(t)k = (1, 2, \ldots, k)$, set the balance parameter $\alpha$, and then initialize.

*Step 2:* The analytical signal that is consistent with the Hilbert transform is calculated via the following equation.

$$A\boldsymbol{u_k}(t) = \boldsymbol{u_k}(t) + \frac{i}{\pi}\int_{-\infty}^{+\infty}\frac{\boldsymbol{u_k}(\tau)}{t-\tau}d\tau = (\delta(t) + \frac{i}{\pi t}) \times \boldsymbol{u_k}(t), \quad i = \sqrt{-1} \tag{1}$$

*Step 3:* The complex exponential term $e^{-if_k t}$ is mixed with the analytical signal $Au_k(t)$ to transfer the spectrum of the mixed signal to a consistent estimated center frequency. Next, a constraint variation problem is formulated:

$$\min_{\{u_k\},\{f_k\}}\left\{\sum_k \left\| \partial t\left[\left(\delta(t) + \frac{i}{\pi t}\right) * \boldsymbol{u_k}(t)\right] e^{-if_k t}\right\|_2^2\right\} \tag{2}$$

$$\sum_k \boldsymbol{u_k}(t) = \boldsymbol{x}(t) \tag{3}$$

Here, $x(t)$ is the raw sequence, $\delta$ represents the Dirac distribution, and $*$ is used to represent the convolution operator.

*Step 4:* Define a new constraint problem as follows:

$$\mathbf{L}\left(\{\boldsymbol{u_k}\}\,\{\boldsymbol{f_k}\}\right) = \alpha\sum_k \left\| \partial t\left[\left(\delta(t) + \frac{i}{\pi t}\right) * \boldsymbol{u_k}(t)\right] e^{-if_k t}\right\|_2^2 + \left\| \boldsymbol{x}(t) - \sum_k \boldsymbol{u_k}(t)\right\|_2^2 + \left\langle \lambda(t), \boldsymbol{x}(t) - \sum_k \boldsymbol{u_k}(t)\right\rangle \tag{4}$$

and

$$f_k^{n+1} = \frac{\int_0^\infty f\left|\hat{\boldsymbol{u}}_{\boldsymbol{k}}(f)\right|^2 df}{\int_0^\infty \left|\hat{\boldsymbol{u}}_{\boldsymbol{k}}(f)\right|^2 df} \tag{5}$$

A more detailed explanation can be found in Ref. [51].

## B. IMMUNE SELECTION MULTI-OBJECTIVE OPTIMIZATION DRAGONFLY ALGORITHM

The dragonfly algorithm (DA) simulates the behavior of the dragonfly population and performs global and local searches [52], [53].

### 1) DRAGONFLY ALGORITHM

**Behavior pattern of group movement of dragonflies:**

Spacing: Avoid collisions between two individuals

$$\boldsymbol{S}_{\rm i} = -\sum_{j=1}^N (X - X_j) \tag{6}$$

Here, $\boldsymbol{S}_i$ is the separation of the $i-th$ individual, and $X$ and $Xj$ represent the positions of two individuals.

Alignment: Keep the movement of oneself in harmony with the movements of other individuals in the group.

$$\boldsymbol{A}_i = \sum_{j=1}^N V_j/N \tag{7}$$

**Algorithm 1** Pseudo Code of the VMD

Select the number of the decomposed modes and the balance parameter $\alpha$. Initialize $\{\hat{u}_k^1\}, \{\hat{f}_k^1\}, \hat{\lambda}, n \leftarrow 0$

**Repeat**

  Start counting $n \leftarrow n + 1$

**FOR** ($k$=1:k) **DO**

/*Decomposing real-valued multi-component signals into modalities*/

Update $\hat{\boldsymbol{u}}_k$ for all $f \geq 0$

$\hat{\boldsymbol{u}}_{\boldsymbol{k}}^{\boldsymbol{n+1}}(f) = \left[\hat{f}(f) - \sum_{i<k}\hat{\boldsymbol{u}}_{\boldsymbol{k}}^{\boldsymbol{n+1}}(f) - \sum_{i>k}\hat{\boldsymbol{u}}_{\boldsymbol{k}}^{\boldsymbol{n}}(f) + \frac{\hat{\lambda}^n(f)}{2}\right] \Big/ [1 + 2\alpha(f - f_k^n)^2$

Update center frequency $\hat{\boldsymbol{f}}_k$ :

$\boldsymbol{f}_{\boldsymbol{n+1}}^{\boldsymbol{k}} = \int_0^\infty f\left|\hat{\boldsymbol{u}}_{\boldsymbol{k}}^{\boldsymbol{n+1}}(f)\right|^2 df \Big/ \int_0^\infty \left|\hat{\boldsymbol{u}}_{\boldsymbol{k}}^{\boldsymbol{n+1}}(f)\right|^2 df$

/*Decomposed mode must be the most compact around its center frequency*/

**END FOR**

Dual ascent for all $f \geq 0$ :

$\hat{\lambda}^{n+1}(f) = \hat{\lambda}^n(f) + \tau\left(\hat{\boldsymbol{f}}(f) - \sum_k \hat{\boldsymbol{u}}_{\boldsymbol{k}}^{\boldsymbol{n+1}}(f)\right)$

/*Until convergence to the specified convergence tolerance criteria*/

**UNTIL convergence:** $\sum_k \left\|\hat{\boldsymbol{u}}_{\boldsymbol{k}}^{\boldsymbol{n+1}} - \hat{\boldsymbol{u}}_{\boldsymbol{k}}^{\boldsymbol{n}}\right\|_2^2 \Big/ \left\|\hat{\boldsymbol{u}}_{\boldsymbol{k}}^{\boldsymbol{n}}\right\|_2^2 < \varepsilon$

where $\boldsymbol{A}_i$ is the alignment quantity and $Vj$ represents the speed of the $j-th$ neighboring individual.

Cohesion: An individual tries to approach a group to which it believes it belongs.

$$\boldsymbol{C}_i = \frac{\sum_{j=1}^N X_j}{N} - X \tag{8}$$

Finding prey: Individual dragonflies finding prey.

$$\boldsymbol{F}_i = X^+ - X \tag{9}$$

Here, $\boldsymbol{F}_i$ represents the attraction of individuals to prey, and $X^+$ denotes the location of the prey.

Avoid enemies: Dragonflies avoid enemies during predation.

$$\boldsymbol{E}_i = X^- + X \tag{10}$$

where $\boldsymbol{E}_i$ is the individual escape distance, and $X^-$ represents the location of the enemy.

**Update process of step and position vectors of dragonflies:**

Step vector $\Delta X_{t+1}$ indicates the direction and step length of a dragonfly:

$$\Delta X_{t+1} = (s\boldsymbol{S}_i + a\boldsymbol{A}_i + c\boldsymbol{C}_i + f\boldsymbol{F}_i + e\boldsymbol{E}_i) + w\Delta\boldsymbol{X}_t \tag{11}$$

The position vector $\boldsymbol{X}_{t+1}$ of a dragonfly is calculated as follows:

$$\boldsymbol{X}_{t+1} = \boldsymbol{X}_t + \Delta\boldsymbol{X}_{t+1} \tag{12}$$

If there is no adjacent solution near the individual, the random walk ($Le'vy$) strategy is used to search in the search space.

$$\boldsymbol{X}_{t+1} = \boldsymbol{X}_t + Le'vy(d) \times \boldsymbol{X}_t \tag{13}$$

Here, $d$ represents the dimension of a single position vector. The $Le'vy$ function is expressed as follows:

$$Le'vy(x) = 0.01 \times \frac{r_1 \times \sigma}{|r_2|^{\frac{1}{\beta}}}, r_1, r_2 = rand(0, 1) \tag{14}$$

$$\sigma = \left( \frac{\Gamma(1+\beta) \times \sin(\frac{\pi\beta}{2})}{\Gamma(\frac{1+\beta}{2}) \times \beta \times 2^{(\frac{\beta-1}{2})}} \right)^{\frac{1}{\beta}}, \Gamma(x) = (x-1)! \tag{15}$$

where $\beta$ is a constant.

### 2) IMMUNE ALGORITHM

The immune algorithm (IA) is based on the principle of biological immunity. The immune system is a complex adaptive system, which can protect the body from external pathogens. It attaches all the cells and molecules of the body to its own species, and divides external sources into non-self molecular species. It can optimize the solution by imitating the process of the biological immune system, which produces an immune response when it fights against foreign antigens and automatically produces corresponding antibodies for destroying invading antigens [54], [55].

IA can effectively maintain the population diversity by utilizing the diversity generation and maintenance mechanisms of the biological immune system, overcome the premature stagnation in the complex optimization process, and yield the globally optimal solution. This avoids the problem that DA method is prone to falling into a local optimum at the end of the optimization iterations and improves the global search performance.

### 3) IMMUNE SELECTION OPERATION FOR THE DRAGONFLY ALGORITHM

During the algorithm optimization stage, if the optimality of successive generations of groups is not significantly improved, then the immune selection operation produces a new population. The implementation steps of the transformed immune selection operation are as follows:

*Step 1:* Calculated the fitness value $FA(X_i)$ of dragonfly $X_i$. The fitness function includes two indicators, one is accuracy and the other is stability, and is defined as: $FA_1 = 1/N \sum_{i=1}^{N} |\hat{y}_i - y_i|$, $FA_2 = std(\hat{y}_i - y_i)$, $y_i$ is the true value, $\hat{y}_i$ is the predicted value.

*Step 2:* Calculate the similarities between dragonfly individuals:

$$D_{ij} = |FA(X_i) - FA(X_j)| \tag{16}$$

$$d_{ij} = \begin{cases} 1, & D_{ij} < \min D \\ 0, & D_{ij} \geq \min D \end{cases} \tag{17}$$

**Algorithm 2** Pseudo Code of the ISMODA

Initialize the dragonfly population with random solutions;
Initialize step vectors $\Delta X_i (i = 1, 2, \cdots, N)$;
Set $DS$=8; (after every DS iteration, check whether the optimal individual has improved)
Set $replaceP$=0.5; (individuals with lower expected reproduction probability than replaceP will be immune replaced)
Set $\min D = 1e - 10$; (the minimum distance between individuals)
Calculate the fitness function for each search agent
Find the nondominated PO solution and initialize the external archive ($A$) with them.
**WHILE** ($t < \boldsymbol{Iter}_{\mathbf{max}}$)
  Calculate the fitness of all dragonflies; Select the best solution as the food source; Select the worst solution as the enemy;
  Update *s, a, c, f, e and w*;
  **FOR** $i = 1: N$
    Calculate $S_i, A_i, C_i, F_i, and\ E_i$;
    Update the neighboring radius;
    **IF** a dragonfly has at least one neighboring dragonfly
      Update the velocity vector and position vector:
      $\Delta X_{t+1} = (sS_i + aA_i + cC_i + fF_i + eE_i) + w\Delta X_t, X_{t+1} = X_t + \Delta X_{t+1}$
    **ELSE**
      Update the position vector via a random walk (*Le'vy* flight):
      $X_{t+1} = X_t + Le'vy(d) \times X_t$
    **END IF**
    Check and correct the new positions based on the boundaries of the variables;
  **END FOR**
  Identify the optimal individual of the current iteration *Xbest(t)*;
  **IF** t $> DS$
    **IF** $\mathrm{mod}(t, DS) == 0 \&\& (Xbest(t - DS + 1)) - Xbest < 1e - 20$
**FOR** i $= 1: N$
    **FOR** j$= 1: N$
    Calculate the distance between each individual and all other individuals and calculate the similarity between individuals: $D_{ij} = |FA(X_i) - FA(X_j)|$ $d_{ij} = \begin{cases} 1, & D_{ij} < \min D \\ 0, & D_{ij} \geq \min D \end{cases}$
  **END FOR**
  Calculate the individual concentration between each individual and calculate the expected reproduction probability;
  $IC_i = \frac{1}{N} \sum_{j=1}^{N} d_{ij} PR(i) = \alpha \frac{FA(X_i)}{\sum_{j=1}^{N} FA(X_j)} + (1-\alpha) \frac{IC_i}{\sum_{j=1}^{N} IC_j}$
  **IF** $PR(i) < replaceP$

**Algorithm 2** *(Continued.)* Pseudo Code of the ISMODA

24: Randomly generated a new individual to replace the original individual i;
25: **END IF**
26: **END FOR**
27: **END IF**
28: **END IF**
29: **t = t+1**
30: **END WHILE** Output the best solution that was found.

where $\min D$ represents the minimum distance between individuals.

*Step 3:* Calculate the individual concentration of *ICi*.

$$IC_i = \frac{1}{N}\sum\nolimits_{j=1}^{N} d_{ij} \tag{18}$$

*Step 4:* Calculate the expected reproduction probabilities of individuals.

$$PR(i) = \alpha\frac{FA(X_i)}{\sum_{j=1}^{N} FA(X_j)} + (1-\alpha)\frac{IC_i}{\sum_{j=1}^{N} IC_j}, \quad \alpha \in \ rand\ (0, 1) \tag{19}$$

*Step 5:* Conduct the immune selection operation on individuals according to their expected reproductive probabilities. If the probability of the current individual is large, the elite retention strategy will be adopted for the individual; if the probability is small, the immune replacement operation will be conducted for the individual.

The expected reproduction probability of an individual is proportional to its fitness value and inversely proportional to its individual concentration. This not only ensures the diversity of individuals but also effectively prevents the iteration from falling into a local optimum and further improves the convergence performance of the algorithm.

## III. DATA PREPROCESSING MODULE

The randomness and complexity of wind energy data lead to inaccurate prediction results. The processing of the raw wind energy data has become an important step in wind speed prediction. To obtain satisfactory prediction values, data preprocessing is necessary. In this section, we introduce a data preprocessing module that uses the VMD strategy to eliminate high-frequency noise signals from the original wind speed sequence, and the strategy of decomposition and reconstruction is used to preprocess the original data.

### A. INFORMATION ON THE ORIGINAL DATASETS

Wind energy resources are widely distributed in northwest, east and northeast China. Shandong (north latitude: 37°48’, east longitude: 120°45’) is a coastal province of China with natural advantages. There are rich wind energy resources and developed wind power industries. Therefore, short-term wind speed datasets of the Shandong Peninsula with a time interval of 10 minutes were collected for the study (as presented in **Fig. 3** and **Table 2**). The humidity and air pressure in this region are 65% and 1012.7 hPa, respectively. The data sites are in mountainous and hilly areas, the altitude ranges from 100 m to 240 m, and the measurement height is 70 m. The researchers found that the spatiotemporal variability of wind resources in China is large. Temporally, the wind resources over all of China are more abundant in the cold season (spring and winter with peaks in April) than in the warm season (summer and autumn with minimal values in August) [56]. To more effectively evaluate the performance of the prediction model, we conducted seasonal data collection. Shandong peninsula has a typical warm temperate monsoon climate. According to its climatic characteristics, we choose the representative month of each season for constructing the dataset: April is the representative month of spring, July is the representative month of summer, October is the representative month of autumn, and January is the representative month of winter. Consider the winter dataset as an example. These data were sampled from January 1, 2011 to January 20, 2011; this period spans 20 days and includes 2880 samplings. We divide each wind speed sequence into two groups: a training sample and a testing sample. This division is illustrated in **Fig. 3**. The data from the initial 16 days, namely, from January 1, 2011 to January 16, 2011, are used as the input for training to establish

**TABLE 2.** Main information characteristics of the raw wind energy data.

| Dataset | Samples | Number | Data | Statistical Indicator(m/s) | | | |
|---|---|---|---|---|---|---|---|
| | | | | Max | Min | Mean | Std. |
| **Spring** | All samples | 2880 | 2011/04/01-2011/04/20 | 19.40 | **0.80** | 7.6302 | 3.2133 |
| | Training samples | 2304 | 2011/04/01-2011/04/16 | 14.70 | **0.80** | 6.8878 | 2.6857 |
| | Testing samples | 576 | 2011/04/17-2011/04/20 | 19.40 | **3.20** | 10.5998 | 3.4300 |
| **Summer** | All samples | 2880 | 2011/07/01-2011/07/20 | 12.50 | **0.90** | 4.8620 | 2.0217 |
| | Training samples | 2304 | 2011/07/01-2011/07/16 | 12.50 | **0.90** | 5.1261 | 2.1017 |
| | Testing samples | 576 | 2011/07/17-2011/07/20 | 8.30 | **1.00** | 3.8056 | 1.1728 |
| **Autumn** | All samples | 2880 | 2011/10/01-2011/10/20 | 13.80 | **0.80** | 5.5087 | 2.3927 |
| | Training samples | 2304 | 2011/10/01-2011/10/16 | 13.80 | **0.80** | 5.6466 | 2.5130 |
| | Testing samples | 576 | 2011/10/17-2011/10/20 | 10.80 | **1.70** | 4.9573 | 1.7299 |
| **Winter** | All samples | 2880 | 2011/01/01-2011/01/20 | 18.10 | **2.30** | 9.4241 | 2.8516 |
| | Training samples | 2304 | 2011/01/01-2011/01/16 | 18.10 | **2.30** | 9.7592 | 2.9562 |
| | Testing samples | 576 | 2011/01/17-2011/01/20 | 12.80 | **2.50** | 8.0837 | 1.8609 |

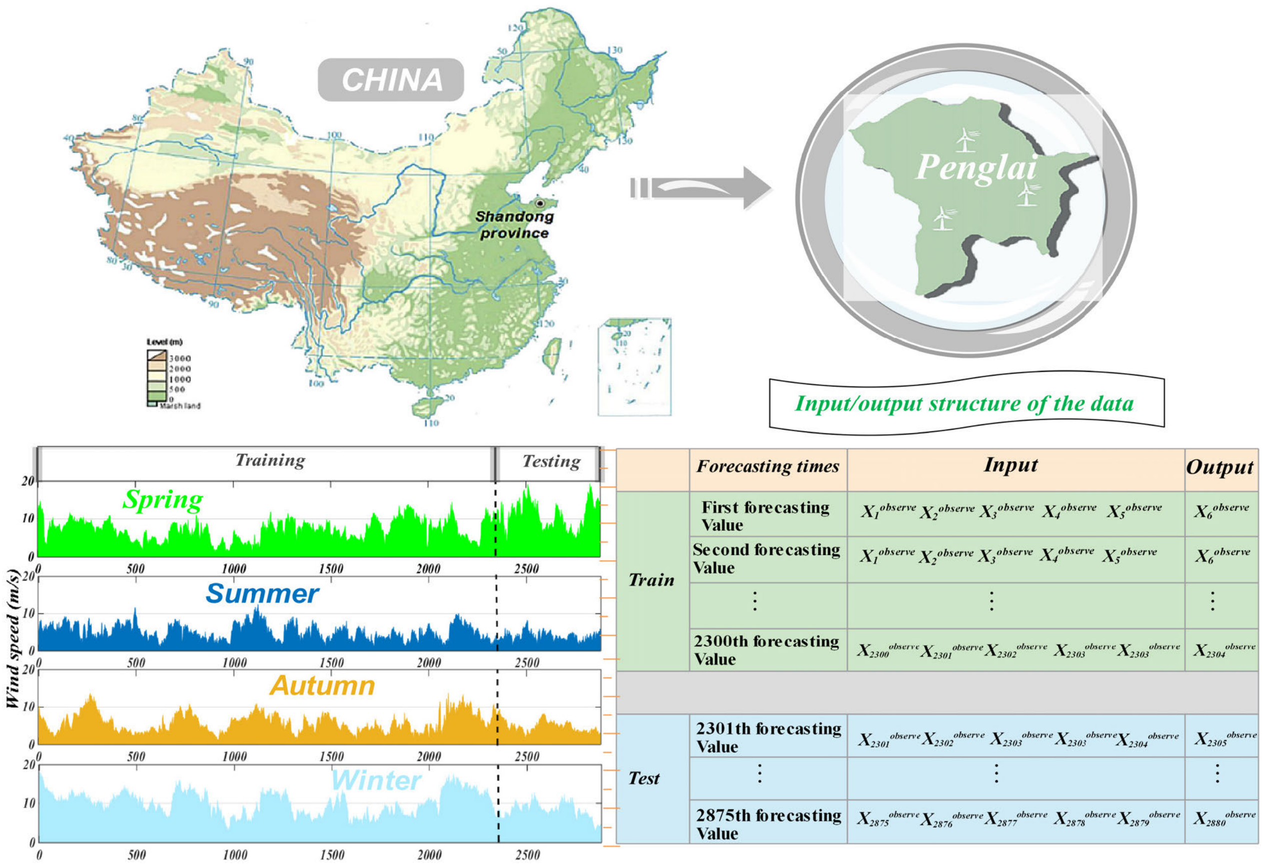


**FIGURE 3.** Information on the original data.

the matrix for the model and the remaining data, namely, the data from January 17, 2011 to January 20, 2011, are used for testing. This same rolling prediction mechanism was used on the training sample and the testing sample.

### B. WIND SPEED SEQUENCE AFTER PROCESSING

In the prediction process, the processing of the original data sequence is necessary. By analyzing the characteristics of the original sequence, the prediction accuracy can be effectively improved. Via the data preprocessing strategy, the original signal is decomposed, and the high-frequency noise signals that affect the prediction are removed and reintegrated into a stable sequence. Based on the integration strategy, the adverse impact of high-frequency noise is eliminated. By this approach, the initial wind speed sequences are reconstructed. Moreover, each reconstructed wind speed sequence extracts the main characteristics of the initial sequence; the instability and randomness of the wind speed sequence are significantly reduced. The prediction performance could be enhanced effectively. The data characteristics of the denoised sequence are listed in **Table 3**. In addition, the reconstructed sequence will be used for future predictions.

**TABLE 3.** Main information characteristics of the wind energy data after processing.

| Dataset | Samples | Number | Statistical Indicator(m/s) | | | |
|---|---|---|---|---|---|---|
| | | | Max | Min | Mean | Std. |
| Spring | All samples | 2880 | 18.31 | **1.01** | 7.6302 | 3.1622 |
| | Training samples | 2304 | 14.33 | **1.01** | 6.8881 | 2.6346 |
| | Testing samples | 576 | 18.31 | **3.83** | 10.5984 | 3.3515 |
| Summer | All samples | 2880 | 12.07 | **1.07** | 4.8620 | 1.9643 |
| | Training samples | 2304 | 12.07 | **1.07** | 5.1258 | 2.0413 |
| | Testing samples | 576 | 7.76 | **1.18** | 3.8070 | 1.1121 |
| Autumn | All samples | 2880 | 12.96 | **1.00** | 5.5087 | 2.3522 |
| | Training samples | 2304 | 12.96 | **1.00** | 5.6466 | 2.4707 |
| | Testing samples | 576 | 10.37 | **1.88** | 4.9573 | 1.6952 |
| Winter | All samples | 2880 | 17.75 | **2.61** | 9.4241 | 2.8067 |
| | Training samples | 2304 | 17.75 | **2.61** | 9.7588 | 2.9107 |
| | Testing samples | 576 | 12.17 | **2.62** | 8.0851 | 1.8064 |

## IV. ACCURACY EVALUATION INDEX AND VALIDITY EVALUATION INDEX

To evaluate the prediction performance of the proposed model, we designed several evaluation indices for testing the accuracy of prediction. On this basis, a discussion module was added to examine the prediction performance of the model in terms of several special evaluation indices. A detailed explanation of these indicators is as follows.

### A. ACCURACY EVALUATION INDEX

Predictive accuracy evaluation is an indispensable part of this research, and multiple performance indicators are used to test the predictive performance of the predictive model. However, there are no systematic regulations regarding evaluation indicators of prediction models. This study uses several commonly used evaluation criteria, namely, MAPE, MAE, RMSE, and SSE, to evaluate the forecasting performance [57].

The MAE and RMSE can be used to represent the average error of the predicted result with respect to the ground-truth result. The total prediction error is represented by SSE. Among the several evaluation indices, the most commonly used index in the application is MAPE, which can be used to evaluate the prediction accuracy of the forecasting model. The criteria are described in detail in **Table 4** [58].

**TABLE 4. Four evaluation criteria.**

| Metric | Definition | Equation |
|---|---|---|
| SSE | sum of error squares | $SSE = \sum_{i=1}^{N}\left(Y_i - \hat{Y}_i\right)^2$ |
| RMSE | square root of average of error squares | $RMSE = \sqrt{\frac{1}{N}\times\sum_{i=1}^{N}\left(Y_i - \hat{Y}_i\right)^2}$ |
| MAE | mean absolute error | $MAE = \frac{1}{N}\sum_{i=1}^{N}\left\|Y_i - \hat{Y}_i\right\|$ |
| MAPE | average of $N$ absolute percentage error | $MAPE = \frac{1}{N}\sum_{i=1}^{N}\left\|Y_i - \hat{Y}_i\right\|/Y_i \times 100\%$ |

### B. TESTING METHODS

The predictive performance of the proposed model is evaluated statistically via the detection of several special indicators.

#### 1) FORECASTING EFFECTIVENESS

The effectiveness of prediction is measured by the sum of the squares of the prediction errors, which is an effective method. In contrast, in this section, we introduce a new scientific validity measure: the mean variance of the prediction accuracy. The index is defined by the following formula [59]:

$A_n$ is the prediction accuracy:

$$A_n = 1 - |\varepsilon_n| \tag{20}$$

$$\varepsilon_n = \begin{cases} -1, & (y_n - \hat{y}_n)/y_n < 1 \\ (y_n - \hat{y}_n)/y_n, & -1 \le (y_n - \hat{y}_n)/y_n < 1 \\ 1, & (y_n - \hat{y}_n)/y_n > 1 \end{cases} \tag{21}$$

The k-order forecasting validity is expressed by the following formula:

$$\mathrm{m_k} = \sum_{n=1}^{N} Q_n A_n^k, \sum_{n=1}^{N} Q_n = 1 \tag{22}$$

The probability distribution is discrete, and its prior information cannot be obtained. We assume it is 1; hence, $Q_n$ is expressed here as *1/N*. $\boldsymbol{H}$ represents a continuous function of a *kth*-order prediction effectiveness element. $\boldsymbol{H}\left(m^1, m^2, \cdots, m^k\right)$is the k-order prediction effectivenesses.

The frist-order and second-order forecasting effectivenesses are expressed as follows:

$$\boldsymbol{H}\left(m^1\right) = m^1 \tag{23}$$

$$\boldsymbol{H}\left(m^1, m^2\right) = m^1\left(1 - \sqrt{m^2 - (m^1)^2}\right) \tag{24}$$

#### 2) DIEBOLD-MARIANO TEST

The DM test is a hypothesis testing method that determines whether the statistical hypothesis of an inference is established by examining the magnitude of the statistic, thereby determining whether the hypothesis is true. This paper uses this method to prove the significant difference among the forecasting results of the combined forecasting system and other models, and more effectively proves the predictive performance of the predictive model [60]. The DM test is introduced as follows [61]:

The error of the predicted results with respect to the ground-truth results is defined by the following formulas:

$$e_{n+h}^1 = y_{n+h} - \hat{y}_{n+h}^1 \tag{25}$$

$$e_{n+h}^2 = y_{n+h} - \hat{y}_{n+h}^2 \tag{26}$$

Here, $y_{n+h}$ and $\hat{y}_{n+h}$ are the ground-truth value and the forecasting result, and $n$ and $h$ represent the number of prediction series and the forecast step size, respectively.

The loss function $\boldsymbol{F}(e_{n+h}^i) i = 1, 2$ is defined for calculating the prediction accuracy. The general method of determining the loss function is as follows:

$$\boldsymbol{F}(e_{n+h}^i) = (e_{n+h}^i)^2 \tag{27}$$

$$\boldsymbol{F}(e_{n+h}^i) = \left|e_{n+h}^i\right| \tag{28}$$

The DM statistic is defined by Eq. (21) as follows:

$$\boldsymbol{DM} = \frac{\frac{1}{T}\sum_{n=1}^{T}(\boldsymbol{F}(e_{n+h}^1) - \boldsymbol{F}(e_{n+h}^2))}{\sqrt{S^2/T}} \tag{29}$$

Here, $S^2$denotes the variance estimate of $\boldsymbol{F}(e_{n+h}^1) - \boldsymbol{F}(e_{n+h}^2)$.

Two prior assumptions are specified: the original hypothesis $H_0$ and the alternative hypothesis $H_1$. The original hypothesis is $H_0 : \boldsymbol{F}(e_{n+h}^1) = \boldsymbol{F}(e_{n+h}^2)$, and the alternative hypothesis is $H_1 : \boldsymbol{F}(e_{n+h}^1) \neq \boldsymbol{F}(e_{n+h}^2)$.

#### 3) GREY RELATIONAL ANALYSIS

By using the grey relational analysis (GRA) index, we can calculate the degree of fit between the predicted values and the ground-truth values, and we can judge whether the predicted sequence is similar to the original sequence. The method is introduced as follows:

The original sequence and forecasting sequence are denoted as

$$X_0 = (X_0(1), X_0(2), \cdots, X_0(n))$$

$$X_i = (X_i(1), X_i(2), \cdots, X_i(n)) \tag{30}$$

The series are standardized by

$$x_i(t) = \frac{X_i(t) - \frac{1}{n}\sum_{t=1}^{n} X_i(t)}{\sqrt{\frac{1}{n-1}\sum_{t=1}^{n}\left(X_i(t) - \frac{1}{n}\sum_{t=1}^{n} X_i(t)\right)}} \tag{31}$$

The correlation between the two sequences is calculated as follows:

$$\xi_i(k) = \frac{\min_i \min_k |x_0(k)-x_i(k)| + \rho \max_i \max_k |x_0(k)-x_i(k)|}{|x_0(k)-x_i(k)| + \rho \max_i \max_k |x_0(k)-x_i(k)|}, \quad \rho \in (0, \infty) \tag{32}$$

The gray correlation degree of the two sequences is calculated as follows:

$$r_i = \frac{1}{n}\sum_{k=1}^{n} \xi_i(k) \tag{33}$$

The value of $r_i$ corresponds to the degree of similarity between the *i-th* prediction curve and the ground-truth curve.

#### 4) DIRECTION OF FORECASTING

To determine whether the data trends of the prediction sequence and the original sequence are consistent, we propose an effective statistic, namely the directivity ($D_{accuracy}$), for evaluating the degree of consistency between the prediction curve and the original curve:

$$D_{accuracy} = \frac{1}{N}\sum_{i=1}^{N} a_i \times 100\% \tag{34}$$

$$\begin{cases} a_i = 1, (y_{i+1} - y_i)(\hat{y}_{i+1} - y_i) \geq 0 \\ a_i = 0, (y_{i+1} - y_i)(\hat{y}_{i+1} - y_i) < 0 \end{cases} \tag{35}$$

Here, $N$ denotes the length of the forecasting curve, $\hat{y}$ is a data point of the prediction sequence, and $y$ is the corresponding data point of the original sequence. $D_{accuracy}$ represents the degree of directional consistency of the two sequences, which is obtained via calculation.

## V. EXPERIMENTAL DESIGN AND RESULTS

Four comparative experiments are designed in this part. The forecasting accuracy of the proposed model is evaluated via these experiments. The experiments were run on the MATLAB 2018 platform.

### A. EXPERIMENT 1: COMBINE MODEL VS. SINGLE MODELS

In this section, the prediction accuracies of the combined model and four single models are compared. The four single models are VMD-ARIMA, VMD-BPNN, VMD-ENN, and VMD-ELM, which are the components that are used to build the combined model. **Table 5** presents the experimental result data, and a more vivid comparison is presented in **Fig. 4**. Then, we interpret the comparison results.

During the wind speed prediction process in the spring, the proposed model realizes the highest forecasting accuracy, regardless of whether it uses single-step prediction or multi-step prediction. The minimum MAPE values are 2.81%, 3.29%, and 3.58%. In the data concentration in the summer, due to the low values of the raw wind speed sequence in the climatic characteristics of wind power sites, the accuracy index was larger than that predicted value in spring. The values of the proposed combined model are 5.02%, 6.08%, and 5.85%. Because the fluctuation of wind speed series in summer is not as strong as that in spring, the SSE index is much smaller than that in spring. The wind speed sequence in autumn is similar to that in summer, and the prediction results of the model are very similar to those in summer. The index values of SSE is 6.5172, 8.8690, and 10.3548, and the

**TABLE 5.** Results of experiment 1.

| Dataset | Model | MAPE (%) | | | MAE | | | RMSE | | | SSE | | |
|---|---|---|---|---|---|---|---|---|---|---|---|---|---|
| | | 1-step | 2-step | 3-step | 1-step | 2-step | 3-step | 1-step | 2-step | 3-step | 1-step | 2-step | 3-step |
| **Spring** | VMD-ARIMA | 4.51 | 4.17 | 4.30 | 0.4256 | 0.3943 | 0.4151 | 0.5564 | 0.5215 | 0.5460 | 44.5737 | 39.1630 | 42.9318 |
| | VMD-BP | 3.20 | 3.66 | 5.99 | 0.3207 | 0.3498 | 0.5834 | 0.4305 | 0.4769 | 0.7743 | 26.6879 | 32.7570 | 86.3287 |
| | VMD-ELM | 3.16 | 3.68 | 6.20 | 0.3176 | 0.3507 | 0.6199 | 0.4247 | 0.4766 | 0.8123 | 25.9781 | 32.7053 | 95.0123 |
| | VMD-ENN | 3.77 | 6.86 | 9.14 | 0.3631 | 0.6608 | 0.9153 | 0.4778 | 0.8737 | 1.1637 | 32.8728 | 109.9160 | 195.0132 |
| | **Combined model** | **2.81** | **3.29** | **3.58** | **0.2814** | **0.3144** | **0.3568** | **0.3935** | **0.4373** | **0.4913** | **22.2917** | **27.5359** | **34.7631** |
| **Summer** | VMD-ARIMA | 8.84 | 8.57 | 8.47 | 0.2828 | 0.2734 | 0.2726 | 0.3495 | 0.3392 | 0.3384 | 17.5899 | 16.5713 | 16.4884 |
| | VMD-BP | 5.59 | 7.14 | 12.20 | 0.1822 | 0.2295 | 0.3895 | 0.2353 | 0.2878 | 0.4876 | 7.9743 | 11.9259 | 34.2435 |
| | VMD-ELM | 5.61 | 7.36 | 12.26 | 0.1827 | 0.2358 | 0.3905 | 0.2364 | 0.2968 | 0.4878 | 8.0472 | 12.6855 | 34.2583 |
| | VMD-ENN | 5.97 | 11.36 | 17.46 | 0.1928 | 0.3630 | 0.5445 | 0.2498 | 0.4479 | 0.6530 | 8.9831 | 28.8856 | 61.4102 |
| | **Combined model** | **5.02** | **6.08** | **5.85** | **0.1632** | **0.2002** | **0.1992** | **0.2181** | **0.2532** | **0.2668** | **6.8523** | **9.2344** | **10.2473** |
| **Autumn** | VMD-ARIMA | 7.63 | 7.44 | 7.32 | 0.2386 | 0.2338 | 0.2296 | 0.3080 | 0.2957 | 0.2927 | 13.6596 | 12.5945 | 12.3340 |
| | VMD-BP | 5.65 | 6.58 | 9.59 | 0.1789 | 0.2074 | 0.3017 | 0.2254 | 0.2659 | 0.3930 | 7.3134 | 10.1785 | 22.2441 |
| | VMD-ELM | 5.69 | 6.59 | 9.43 | 0.1794 | 0.2080 | 0.2961 | 0.2258 | 0.2652 | 0.3854 | 7.3402 | 10.1294 | 21.3935 |
| | VMD-ENN | 7.06 | 9.60 | 11.12 | 0.2241 | 0.3012 | 0.3406 | 0.2915 | 0.3902 | 0.4436 | 12.2336 | 21.9205 | 28.3360 |
| | **Combined model** | **5.05** | **6.15** | **6.74** | **0.1632** | **0.1945** | **0.2153** | **0.2127** | **0.2482** | **0.2682** | **6.5172** | **8.8690** | **10.3548** |
| **Winter** | VMD-ARIMA | 3.56 | 3.43 | 3.93 | 0.2139 | 0.2074 | 0.2329 | 0.2955 | 0.2797 | 0.3095 | 12.5775 | 11.2665 | 13.7977 |
| | VMD-BP | 2.90 | 3.81 | 6.50 | 0.1769 | 0.2249 | 0.3695 | 0.2324 | 0.2827 | 0.4747 | 7.7761 | 11.5097 | 32.4456 |
| | VMD-ELM | 3.14 | 4.01 | 6.35 | 0.1851 | 0.2348 | 0.3639 | 0.2393 | 0.2943 | 0.4707 | 8.2434 | 12.4726 | 31.9025 |
| | VMD-ENN | 3.83 | 7.29 | 10.82 | 0.2114 | 0.3978 | 0.5573 | 0.2658 | 0.4905 | 0.7034 | 10.1773 | 34.6431 | 71.2407 |
| | **Combined model** | **2.46** | **2.60** | **3.40** | **0.1497** | **0.1599** | **0.2087** | **0.1944** | **0.2094** | **0.2668** | **5.4428** | **6.3131** | **10.2535** |

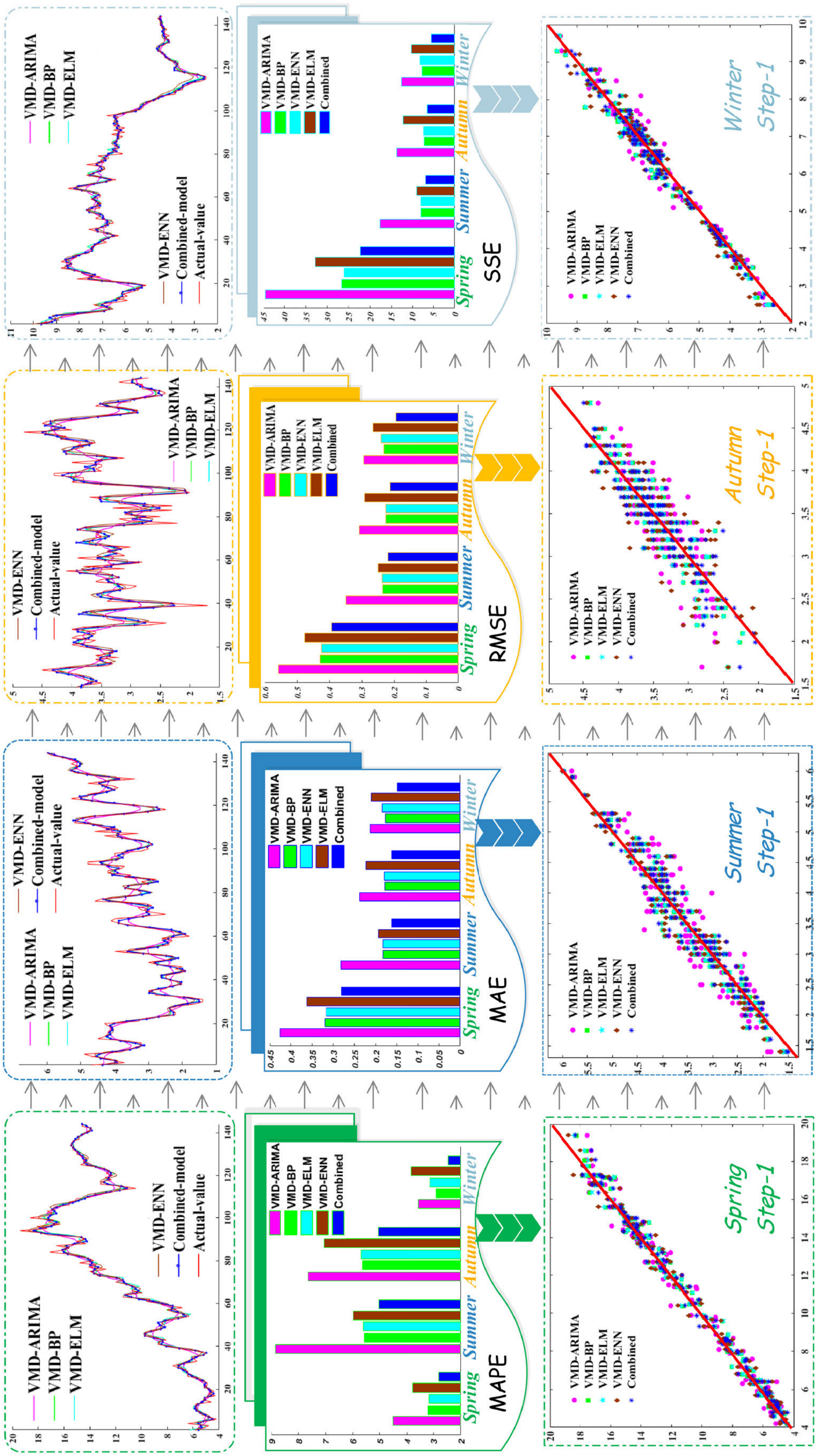


**FIGURE 4.** Results of experiment 1.

**TABLE 6.** Results of experiment 2.

| Dataset | Model | MAPE (%) | | | MAE | | | RMSE | | | SSE | | |
|---|---|---|---|---|---|---|---|---|---|---|---|---|---|
| | | 1-step | 2-step | 3-step | 1-step | 2-step | 3-step | 1-step | 2-step | 3-step | 1-step | 2-step | 3-step |
| **Spring** | ARIMA | 6.67 | 6.73 | 6.82 | 0.6428 | 0.6482 | 0.6596 | 0.8387 | 0.8458 | 0.8535 | 101.2966 | 103.0051 | 104.8865 |
| | BP | 6.65 | 9.28 | 10.83 | 0.6582 | 0.9029 | 1.0954 | 0.8640 | 1.1384 | 1.4119 | 107.4992 | 186.6228 | 287.0458 |
| | ELM | 6.52 | 9.00 | 10.47 | 0.6362 | 0.8666 | 1.0460 | 0.8316 | 1.1240 | 1.3621 | 99.5899 | 181.9250 | 267.1734 |
| | ENN | 6.41 | 9.15 | 11.18 | 0.6306 | 0.8795 | 1.1433 | 0.8170 | 1.1219 | 1.4351 | 96.1251 | 181.2386 | 296.5688 |
| | **Combined model** | **2.81** | **3.29** | **3.58** | **0.2814** | **0.3144** | **0.3568** | **0.3935** | **0.4373** | **0.4913** | **22.2917** | **27.5359** | **34.7631** |
| **Summer** | ARIMA | 12.04 | 11.57 | 11.34 | 0.3966 | 0.3812 | 0.3759 | 0.5127 | 0.4920 | 0.4901 | 37.8451 | 34.8579 | 34.5917 |
| | BP | 11.43 | 17.62 | 21.79 | 0.3751 | 0.5623 | 0.6741 | 0.4869 | 0.6804 | 0.8056 | 34.1437 | 66.6697 | 93.4627 |
| | ELM | 11.30 | 17.52 | 21.49 | 0.3689 | 0.5599 | 0.6717 | 0.4793 | 0.6778 | 0.7997 | 33.0768 | 66.1612 | 92.0901 |
| | ENN | 11.15 | 17.62 | 21.54 | 0.3671 | 0.5631 | 0.6715 | 0.4827 | 0.6799 | 0.7992 | 33.5491 | 66.5659 | 91.9842 |
| | **Combined model** | **5.02** | **6.08** | **5.85** | **0.1632** | **0.2002** | **0.1992** | **0.2181** | **0.2532** | **0.2668** | **6.8523** | **9.2344** | **10.2473** |
| **Autumn** | ARIMA | 11.66 | 10.62 | 10.64 | 0.3664 | 0.3342 | 0.3351 | 0.4782 | 0.4351 | 0.4388 | 32.9324 | 27.2663 | 27.7233 |
| | BP | 10.56 | 14.34 | 14.39 | 0.3292 | 0.4391 | 0.4401 | 0.4321 | 0.5793 | 0.5765 | 26.8884 | 48.3207 | 47.8517 |
| | ELM | 10.63 | 14.09 | 14.33 | 0.3309 | 0.4340 | 0.4365 | 0.4362 | 0.5662 | 0.5727 | 27.4031 | 46.1663 | 47.2266 |
| | ENN | 10.57 | 14.06 | 14.48 | 0.3284 | 0.4353 | 0.4416 | 0.4347 | 0.5653 | 0.5794 | 27.2126 | 46.0109 | 48.3344 |
| | **Combined model** | **5.05** | **6.15** | **6.74** | **0.1632** | **0.1945** | **0.2153** | **0.2127** | **0.2482** | **0.2682** | **6.5172** | **8.8690** | **10.3548** |
| **Winter** | ARIMA | 7.10 | 5.55 | 5.54 | 0.4270 | 0.3361 | 0.3374 | 0.5548 | 0.4375 | 0.4375 | 44.3158 | 27.5623 | 27.5604 |
| | BP | 6.26 | 8.06 | 10.11 | 0.3608 | 0.4527 | 0.5584 | 0.4485 | 0.5925 | 0.7235 | 28.9689 | 50.5464 | 75.3872 |
| | ELM | 5.60 | 8.73 | 10.34 | 0.3358 | 0.4794 | 0.5708 | 0.4278 | 0.6192 | 0.7327 | 26.3503 | 55.2108 | 77.3167 |
| | ENN | 6.40 | 8.60 | 11.15 | 0.3655 | 0.4838 | 0.5990 | 0.4571 | 0.6173 | 0.7626 | 30.0888 | 54.8643 | 83.7531 |
| | **Combined model** | **2.46** | **2.60** | **3.40** | **0.1497** | **0.1599** | **0.2087** | **0.1944** | **0.2094** | **0.2668** | **5.4428** | **6.3131** | **10.2535** |

accuracy of this prediction performance is very similar that in summer. Winter differs from the other three seasons. The wind energy resources in winter are equally abundant as in spring, but the fluctuation of the wind speed series is not as strong as in spring, which leads to very good performance in terms of both the MAPE index and the SSE index.

*Remark 1:* By analyzing the prediction results that are presented above, we conclude that our combined model, namely, VMD-ISMODA, has higher prediction accuracy than the single models that are based on VMD method (VMD-ARIMA, VMD-BP, VMD-ELM, and VMD-ENN). According to the four predictive index values, our proposed combined model yields satisfactory prediction results in multi-step prediction.

### B. EXPERIMENT 2: COMBINED MODEL VS. TRADITIONAL MODELS

In this section, the prediction accuracies of the VMD-ISMODA model and the traditional models are compared experimentally. The four single traditional models are ARIMA, BP, ENN, and ELM, which are the components that are used to build the combined model. **Table 6** shows the experimental result data. Then, we interpret the comparison results.

The seasonal performance is similar to that in experiment 1. The prediction accuracies for spring and winter are relatively high, namely, the MAPE index has low values, and the prediction accuracies for summer and autumn are relatively low. In the prediction results of the spring wind speed series, the BP model performs the worst among the four traditional models. There is a large difference between the one-step prediction and multi-step prediction performances of the ARIMA model: The one-step prediction performance is worse than those of the other traditional models in terms of accuracy, while the multi-step prediction performance is better. During the prediction of the summer wind speed dataset, when forecasting in one step, the prediction performances of the four traditional methods from good to bad are ENN, ELM, BP, and ARIMA, with MAPE values of 11.15%, 11.30%, 11.43% and 12.04%, respectively. The wind speed sequence in autumn is similar to that in summer, and the prediction results of the model are very similar to those in summer. For the winter dataset prediction, the proposed combined model realizes the optimal prediction accuracy.

*Remark 2:* Through the above analysis and the experimental results in **Table 6**, we conclude that the combined VMD-ISMODA model realizes higher prediction accuracy than the traditional models and can realize superior prediction performance.

### C. EXPERIMENT 3: VARIATIONAL MODE DECOMPOSITION VS. OTHER PROCESSING STRATEGIES

This experimental study aims at evaluating the performance of the variational mode decomposition strategy (VMD), in comparison with other widely used decomposition strategies. **Table 7** and **Fig. 5** show the prediction results; the best decomposition methods for various prediction models are identified. From **Table 7** and **Fig. 5**, the following conclusions are drawn:

Data processing strategies that are combined with the same optimization algorithms differ in terms of forecasting accuracy; hence, the data preprocessing method that is used in a combined forecasting system substantially influences the prediction accuracy. According to the results of the four predictive indicators, which are presented in **Table 7**, the performances of the two processing strategies (EMD and EEMD) in the dataset for each season are highly similar; however, compared with the CEEMD strategy, a large gap is observed.

**TABLE 7. Results of experiment 3.**

| Dataset | Model | MAPE (%) | | | MAE | | | RMSE | | | SSE | | |
|---|---|---|---|---|---|---|---|---|---|---|---|---|---|
| | | 1-step | 2-step | 3-step | 1-step | 2-step | 3-step | 1-step | 2-step | 3-step | 1-step | 2-step | 3-step |
| Spring | EMD-Combined | 3.74 | 4.05 | 4.76 | 0.3518 | 0.3762 | 0.4577 | 0.4349 | 0.4895 | 0.6094 | 27.2338 | 34.5038 | 53.4785 |
| | EEMD-Combined | 3.69 | 4.06 | 4.45 | 0.3484 | 0.3721 | 0.4229 | 0.4441 | 0.4873 | 0.5512 | 28.4044 | 34.1936 | 43.7440 |
| | CEEMD-Combined | 3.32 | 3.78 | 4.30 | 0.3342 | 0.3700 | 0.4494 | 0.4464 | 0.4754 | 0.6045 | 28.6992 | 32.5418 | 52.6119 |
| | **Combined model** | **2.81** | **3.29** | **3.58** | **0.2814** | **0.3144** | **0.3568** | **0.3935** | **0.4373** | **0.4913** | **22.2917** | **27.5359** | **34.7631** |
| Summer | EMD-Combined | 7.23 | 8.30 | 8.75 | 0.2480 | 0.2873 | 0.3001 | 0.3043 | 0.3491 | 0.3656 | 13.3372 | 17.5523 | 19.2467 |
| | EEMD-Combined | 7.50 | 8.14 | 8.63 | 0.2540 | 0.2807 | 0.2962 | 0.3064 | 0.3360 | 0.3602 | 13.5153 | 16.2562 | 18.6794 |
| | CEEMD-Combined | 6.26 | 6.80 | 6.40 | 0.1978 | 0.2117 | 0.2158 | 0.2520 | 0.2673 | 0.2905 | 9.1433 | 10.2913 | 12.1497 |
| | **Combined model** | **5.02** | **6.08** | **5.85** | **0.1632** | **0.2002** | **0.1992** | **0.2181** | **0.2532** | **0.2668** | **6.8523** | **9.2344** | **10.2473** |
| Autumn | EMD-Combined | 6.64 | 6.91 | 7.19 | 0.2134 | 0.2275 | 0.2332 | 0.2597 | 0.2865 | 0.3021 | 9.7094 | 11.8182 | 13.1390 |
| | EEMD-Combined | 6.89 | 7.03 | 7.30 | 0.2202 | 0.2212 | 0.2388 | 0.2708 | 0.2742 | 0.3022 | 10.5567 | 10.8300 | 13.1494 |
| | CEEMD-Combined | 6.10 | 6.85 | 7.06 | 0.1901 | 0.2128 | 0.2243 | 0.2404 | 0.2711 | 0.2805 | 8.3241 | 10.5843 | 11.3338 |
| | **Combined model** | **5.05** | **6.15** | **6.74** | **0.1632** | **0.1945** | **0.2153** | **0.2127** | **0.2482** | **0.2682** | **6.5172** | **8.8690** | **10.3548** |
| Winter | EMD-Combined | 3.14 | 3.64 | 3.87 | 0.1962 | 0.2209 | 0.2340 | 0.2504 | 0.2720 | 0.2995 | 9.0315 | 10.6552 | 12.9154 |
| | EEMD-Combined | 3.04 | 3.65 | 3.90 | 0.1840 | 0.2194 | 0.2311 | 0.2419 | 0.2785 | 0.3002 | 8.4247 | 11.1718 | 12.9799 |
| | CEEMD-Combined | 2.83 | 3.45 | 3.82 | 0.1675 | 0.2069 | 0.2298 | 0.2110 | 0.2696 | 0.2908 | 6.4084 | 10.4680 | 12.1753 |
| | **Combined model** | **2.46** | **2.60** | **3.40** | **0.1497** | **0.1599** | **0.2087** | **0.1944** | **0.2094** | **0.2668** | **5.4428** | **6.3131** | **10.2535** |

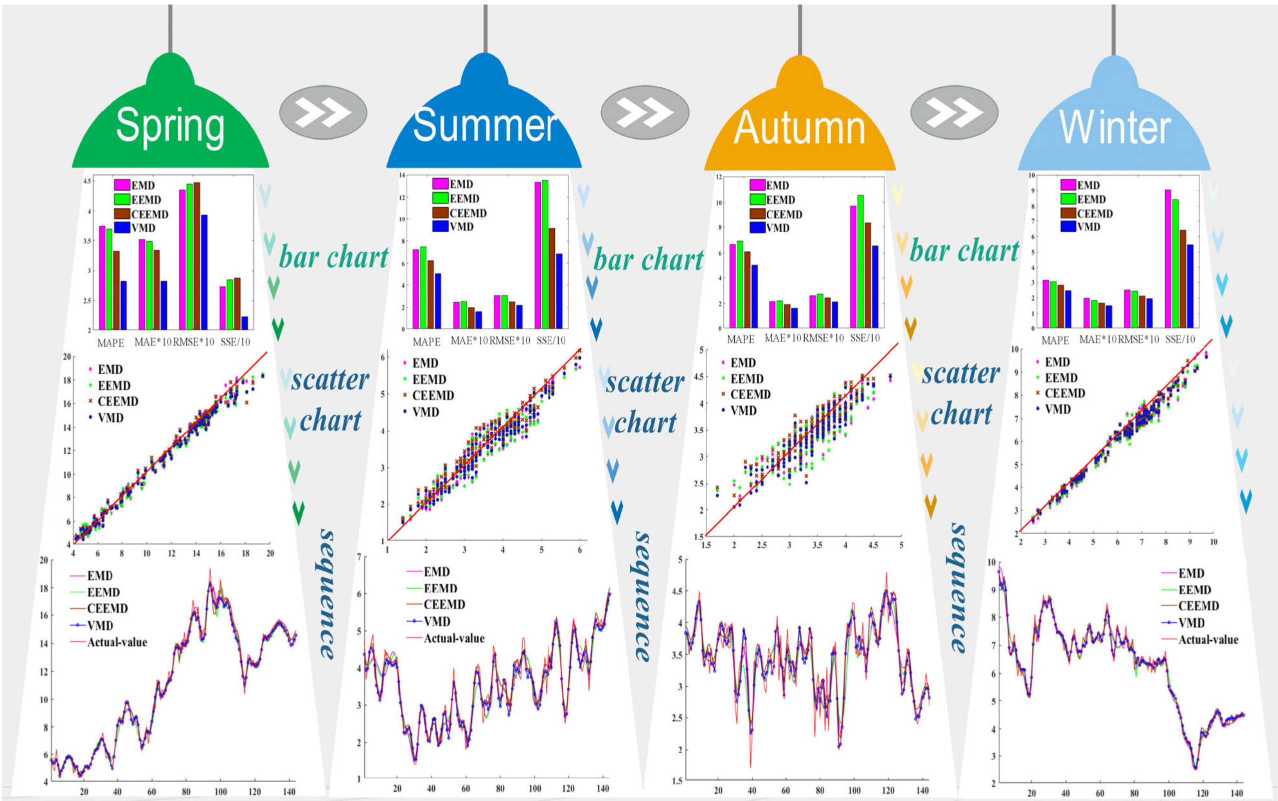


**FIGURE 5. Results of experiment 3.**

The CEEMD strategy outperforms the EMD and EMD strategies in terms of accuracy and stability. In addition, the VMD strategy that is used in our combined model realizes higher precision. Among the selected data preprocessing strategies, the VMD strategy yields the most accurate prediction values.

*Remark 3:* According the above experimental analysis and the values of the prediction indicators in Table 7, the proposed forecasting system, which is based on VMD data processing strategy, can yield excellent forecasting results.

### *D. EXPERIMENT 4: IMMUNE SELECTION MULTI-OBJECTIVE DRAGONFLY VS. OTHER OPTIMIZATION ALGORITHMS*

To evaluate the performance of the ISMODA method, three additional weight determination methods, namely,

**TABLE 8.** Results of experiment 4.

| Dataset | Model | MAPE (%) | | | MAE | | | RMSE | | | SSE | | |
|---|---|---|---|---|---|---|---|---|---|---|---|---|---|
| | | 1-step | 2-step | 3-step | 1-step | 2-step | 3-step | 1-step | 2-step | 3-step | 1-step | 2-step | 3-step |
| Spring | CS-Combined | 3.07 | 3.73 | 4.42 | 0.3017 | 0.3704 | 0.4547 | 0.4141 | 0.5026 | 0.5819 | 24.6872 | 36.3776 | 48.7648 |
| | FA-Combined | 3.10 | 3.65 | 4.40 | 0.3274 | 0.3589 | 0.4306 | 0.4908 | 0.4926 | 0.5659 | 34.6913 | 34.9473 | 46.1084 |
| | MODA-Combined | 2.96 | 3.48 | 3.94 | 0.2925 | 0.3433 | 0.3962 | 0.3891 | 0.4463 | 0.5227 | 21.8045 | 28.6855 | 39.3497 |
| | **ISMODA-Combined** | **2.81** | **3.29** | **3.58** | **0.2814** | **0.3144** | **0.3568** | **0.3935** | **0.4373** | **0.4913** | **22.2917** | **27.5359** | **34.7631** |
| Summer | CS-Combined | 5.57 | 6.79 | 6.95 | 0.1829 | 0.2253 | 0.2433 | 0.2366 | 0.2816 | 0.3146 | 8.0609 | 11.4150 | 14.2555 |
| | FA-Combined | 5.61 | 6.87 | 6.94 | 0.1863 | 0.2278 | 0.2329 | 0.2378 | 0.2813 | 0.3010 | 8.1419 | 11.3922 | 13.0437 |
| | MODA-Combined | 5.46 | 6.46 | 6.26 | 0.1793 | 0.2040 | 0.2153 | 0.2308 | 0.2590 | 0.2875 | 7.6674 | 9.6574 | 11.9045 |
| | **ISMODA-Combined** | **5.02** | **6.08** | **5.85** | **0.1632** | **0.2002** | **0.1992** | **0.2181** | **0.2532** | **0.2668** | **6.8523** | **9.2344** | **10.2473** |
| Autumn | CS-Combined | 5.59 | 6.45 | 7.21 | 0.1754 | 0.2073 | 0.2325 | 0.2227 | 0.2591 | 0.2852 | 7.1420 | 9.6635 | 11.7155 |
| | FA-Combined | 5.60 | 6.44 | 7.21 | 0.1791 | 0.2023 | 0.2374 | 0.2268 | 0.2583 | 0.3000 | 7.4103 | 9.6053 | 12.9633 |
| | MODA-Combined | 5.52 | 6.37 | 7.06 | 0.1754 | 0.2013 | 0.2294 | 0.2227 | 0.2532 | 0.2903 | 7.1402 | 9.2299 | 12.1368 |
| | **ISMODA-Combined** | **5.05** | **6.15** | **6.74** | **0.1632** | **0.1945** | **0.2153** | **0.2127** | **0.2482** | **0.2682** | **6.5172** | **8.8690** | **10.3548** |
| Winter | CS-Combined | 2.74 | 3.13 | 3.92 | 0.1694 | 0.1898 | 0.2306 | 0.2238 | 0.2348 | 0.2861 | 7.2105 | 7.9414 | 11.7843 |
| | FA-Combined | 2.76 | 3.34 | 3.88 | 0.1674 | 0.1984 | 0.2286 | 0.2167 | 0.2584 | 0.2953 | 6.7640 | 9.6123 | 12.5608 |
| | MODA-Combined | 2.72 | 2.96 | 3.73 | 0.1615 | 0.1778 | 0.2206 | 0.1998 | 0.2247 | 0.2796 | 5.7509 | 7.2714 | 11.2596 |
| | **ISMODA-Combined** | **2.46** | **2.60** | **3.40** | **0.1497** | **0.1599** | **0.2087** | **0.1944** | **0.2094** | **0.2668** | **5.4428** | **6.3131** | **10.2535** |

**TABLE 9.** Results of hypothesis testing.

| Model | Spring | | | Summer | | | Autumn | | | Winter | | |
|---|---|---|---|---|---|---|---|---|---|---|---|---|
| | 1-step | 2-step | 3-step | 1-step | 2-step | 3-step | 1-step | 2-step | 3-step | 1-step | 2-step | 3-step |
| VMD-ARIMA | $4.43^{a}$ | $2.86^{a}$ | $2.03^{b}$ | $5.41^{a}$ | $5.95^{a}$ | $4.77^{a}$ | $4.35^{a}$ | $2.99^{a}$ | $2.00^{a}$ | $3.77^{a}$ | $2.89^{a}$ | $2.23^{b}$ |
| VMD-BP | $1.70^{c}$ | $1.91^{c}$ | $4.92^{a}$ | $1.68^{c}$ | $2.85^{a}$ | $6.54^{a}$ | $1.71^{c}$ | 2.72 | $4.62^{a}$ | 2.36 | $4.32^{a}$ | $4.82^{a}$ |
| VMD-ELM | $1.71^{c}$ | $1.83^{c}$ | $5.32^{a}$ | $1.82^{c}$ | $3.40^{a}$ | $6.61^{a}$ | $1.71^{c}$ | 2.63 | $4.44^{a}$ | $2.82^{a}$ | $4.82^{a}$ | $4.62^{a}$ |
| VMD-ENN | $3.14^{a}$ | $6.02^{a}$ | $6.70^{a}$ | $2.00^{a}$ | $7.27^{a}$ | $8.82^{a}$ | $4.47^{a}$ | $5.38^{a}$ | $4.68^{a}$ | $5.00^{a}$ | $6.52^{a}$ | $6.63^{a}$ |
| ARIMA | $6.52^{a}$ | $6.81^{a}$ | $5.82^{a}$ | $7.10^{a}$ | $6.96^{a}$ | $6.38^{a}$ | $6.71^{a}$ | $6.28^{a}$ | $5.40^{a}$ | $6.99^{a}$ | $6.65^{a}$ | $5.60^{a}$ |
| BP | $6.69^{a}$ | $7.35^{a}$ | $6.36^{a}$ | $6.99^{a}$ | $9.27^{a}$ | $8.95^{a}$ | $6.38^{a}$ | $6.28^{a}$ | $5.50^{a}$ | $8.01^{a}$ | $5.66^{a}$ | $6.11^{a}$ |
| ELM | $6.68^{a}$ | $6.86^{a}$ | $6.66^{a}$ | $6.95^{a}$ | $9.28^{a}$ | $8.90^{a}$ | $6.52^{a}$ | $6.23^{a}$ | $5.60^{a}$ | $6.99^{a}$ | $5.92^{a}$ | $6.27^{a}$ |
| EMD | $6.21^{a}$ | $7.36^{a}$ | $7.49^{a}$ | $6.76^{a}$ | $9.37^{a}$ | $8.96^{a}$ | $6.36^{a}$ | $6.51^{a}$ | $5.63^{a}$ | $7.17^{a}$ | $5.95^{a}$ | $6.70^{a}$ |
| EMD | $1.49^{d}$ | $1.58^{d}$ | $2.39^{b}$ | $4.40^{a}$ | $5.48^{a}$ | $4.88^{a}$ | $3.27^{a}$ | $1.88^{c}$ | $1.52^{d}$ | $2.78^{a}$ | $3.16^{a}$ | $1.47^{d}$ |
| EEMD | $1.88^{c}$ | $1.55^{d}$ | $1.43^{e}$ | $5.07^{a}$ | $5.58^{a}$ | $4.82^{a}$ | $3.80^{a}$ | $1.73^{c}$ | $1.64^{c}$ | $2.35^{b}$ | $3.38^{a}$ | $1.65^{c}$ |
| CEEMD | $1.75^{c}$ | $1.54^{a}$ | $3.58^{a}$ | $1.83^{a}$ | $1.65^{a}$ | $2.15^{b}$ | $2.93^{a}$ | $2.84^{a}$ | $1.83^{a}$ | $2.32^{a}$ | $3.11^{a}$ | $1.92^{c}$ |
| CS | $1.91^{c}$ | $2.55^{b}$ | $3.41^{a}$ | 0.94 | $3.79^{a}$ | $3.72^{a}$ | $1.30^{e}$ | $1.41^{e}$ | $2.13^{b}$ | $2.13^{b}$ | $3.22^{a}$ | $1.76^{c}$ |
| FA | $1.66^{c}$ | $2.27^{b}$ | $2.57^{a}$ | $1.19^{f}$ | $3.93^{a}$ | $3.47^{a}$ | $2.15^{a}$ | $1.72^{c}$ | $2.49^{b}$ | $2.91^{a}$ | $2.96^{a}$ | $1.62^{d}$ |
| MODA | $1.34^{e}$ | $1.29^{e}$ | $1.28^{e}$ | $1.33^{a}$ | 1.04 | $2.20^{a}$ | $1.85^{a}$ | 1.14 | $2.21^{a}$ | $1.26^{f}$ | $2.72^{a}$ | $2.51^{a}$ |

[a] is the 1% significance level $Z_{0.01/2}$= 2.58; [b] is the 5% significance level $Z_{0.05/2}=1.96$; [c] is the 10% significance level $Z_{0.10/2}=1.64$; [d] is the 15% significance level $Z_{0.15/2}=1.44$; [e] is the 20% significance level $Z_{0.20/2}=1.28$; [f] is the 25% significance level $Z_{0.25/2}=1.15$.

the cuckoo search algorithm (CS), the firefly algorithm (FA), and the multi-objective dragonfly algorithm (MODA), are used in combination with the VMD data preprocessing strategy for comparison. In addition, The results of the forecast indicators are presented in **Table 8**, and the value for the ISMODA algorithm result is marked in bold.

The weight determination method structures with the VMD data preprocessing strategy differ in terms of prediction performance; hence, the weight determination method in the combined model plays a vital role in improving the performance in wind power forecasting. According to the experimental prediction results that are presented in **Table 8**, the performances of the two single-objective algorithms (CS and FA) in each season are very similar; however, compared with the multi-objective optimization methods (MODA and ISMODA), a large gap is observed. Multi-objective methods are superior to single-objective methods in terms of accuracy and stability. Moreover, our developed multi-objective method (ISMODA) outperforms the original multi-objective algorithm (MODA) in forecasting.

*Remark 4:* From the above experimental analysis and the prediction results that are presented in **Table 8**, we conclude that the proposed multi-objective optimization algorithm (ISMODA) has made outstanding contributions to wind speed prediction and has yielded satisfactory prediction results.

## VI. DISCUSSIONS

In this section, several necessary tests have been conducted to further evaluate the forecasting performance of the proposed VMD-ISMODA prediction system.

### A. RESULTS OF HYPOTHESIS TESTING

The predictive performance of the developed model is tested with the DM test, and the validity of the proposed model, which is based on statistical concepts, is further evaluated. We evaluated other models and the proposed combined model; the results of the DM test are presented in **Table 9** and are briefly described below.

**TABLE 10. Forecasting effectiveness results.**

| Model | Spring | | | | | | Summer | | | | | | Autumn | | | | | | Winter | | | | | |
|---|---|---|---|---|---|---|---|---|---|---|---|---|---|---|---|---|---|---|---|---|---|---|---|---|
| | 1-step | | 2-step | | 3-step | | 1-step | | 2-step | | 3-step | | 1-step | | 2-step | | 3-step | | 1-step | | 2-step | | 3-step | |
| | order-1 | order-2 | order-1 | order-2 | order-1 | order-2 | order-1 | order-2 | order-1 | order-2 | order-1 | order-2 | order-1 | order-2 | order-1 | order-2 | order-1 | order-2 | order-1 | order-2 | order-1 | order-2 | order-1 | order-2 |
| **Combined** | 97.19% | 94.49% | 96.71% | 93.61% | 96.42% | 93.22% | 95.59% | 91.25% | 93.92% | 89.27% | 94.15% | 89.13% | 94.95% | 90.11% | 93.85% | 88.04% | 93.26% | 87.56% | 97.54% | 95.58% | 97.40% | 95.42% | 96.60% | 93.97% |
| **VMD-ARIMA** | 95.49% | 91.40% | 95.83% | 92.17% | 95.70% | 92.02% | 91.16% | 84.62% | 91.43% | 84.97% | 91.53% | 85.21% | 92.37% | 84.73% | 92.56% | 85.34% | 92.68% | 85.67% | 96.44% | 93.26% | 96.57% | 93.72% | 96.07% | 92.79% |
| **VMD-BP** | 96.80% | 94.14% | 96.34% | 92.74% | 94.01% | 88.59% | 94.41% | 89.82% | 92.86% | 87.10% | 87.80% | 78.53% | 94.35% | 89.02% | 93.42% | 87.36% | 90.41% | 81.62% | 97.10% | 94.65% | 96.19% | 93.18% | 93.50% | 87.96% |
| **VMD-ELM** | 96.84% | 94.18% | 96.32% | 92.70% | 93.80% | 88.42% | 94.39% | 89.72% | 92.64% | 86.79% | 87.74% | 78.34% | 94.31% | 88.93% | 93.41% | 87.40% | 90.57% | 81.86% | 96.86% | 94.16% | 95.99% | 92.82% | 93.65% | 88.32% |
| **VMD-ENN** | 96.23% | 92.84% | 93.14% | 87.53% | 90.86% | 84.32% | 94.03% | 88.90% | 88.64% | 79.83% | 82.54% | 70.64% | 92.94% | 86.19% | 90.40% | 81.24% | 88.88% | 77.80% | 96.17% | 92.35% | 92.71% | 86.28% | 89.18% | 78.99% |
| **ARIMA** | 93.33% | 87.75% | 93.27% | 87.65% | 93.18% | 87.61% | 87.96% | 79.20% | 88.43% | 80.00% | 88.66% | 80.26% | 88.34% | 77.48% | 89.38% | 79.42% | 89.36% | 79.34% | 92.90% | 87.46% | 94.45% | 90.10% | 94.46% | 90.22% |
| **BP** | 93.35% | 87.90% | 90.72% | 83.44% | 89.17% | 81.71% | 88.57% | 79.84% | 82.38% | 70.86% | 78.21% | 63.97% | 89.44% | 79.34% | 85.71% | 72.16% | 85.74% | 72.32% | 93.74% | 88.49% | 91.94% | 84.86% | 89.89% | 80.91% |
| **ELM** | 93.48% | 88.16% | 91.00% | 83.66% | 89.53% | 81.97% | 88.70% | 79.97% | 82.48% | 70.98% | 78.51% | 64.78% | 89.37% | 79.19% | 85.96% | 72.89% | 85.79% | 72.28% | 94.40% | 90.08% | 91.27% | 83.34% | 89.66% | 80.98% |
| **ENN** | 93.59% | 88.47% | 90.85% | 83.50% | 88.82% | 81.42% | 88.85% | 80.08% | 82.38% | 70.97% | 78.46% | 64.61% | 89.43% | 79.18% | 85.95% | 72.95% | 85.65% | 72.11% | 93.60% | 88.49% | 91.40% | 84.23% | 88.85% | 78.97% |
| **EMD-Combined** | 96.26% | 93.18% | 95.95% | 92.39% | 95.24% | 91.16% | 92.77% | 87.98% | 91.70% | 86.58% | 91.25% | 85.51% | 93.36% | 88.15% | 93.09% | 87.69% | 92.81% | 86.95% | 96.86% | 94.70% | 96.36% | 93.86% | 96.13% | 93.20% |
| **EEMD-Combined** | 96.31% | 93.08% | 95.94% | 92.25% | 95.55% | 91.73% | 92.50% | 87.81% | 91.86% | 87.05% | 91.37% | 85.89% | 93.11% | 87.51% | 92.97% | 87.04% | 92.70% | 86.93% | 96.96% | 94.66% | 96.35% | 93.59% | 96.10% | 92.66% |
| **CEEMD-Combined** | 96.68% | 93.80% | 96.22% | 93.13% | 95.70% | 92.15% | 93.74% | 88.43% | 93.20% | 87.67% | 93.60% | 87.97% | 93.90% | 88.23% | 93.15% | 86.77% | 92.94% | 86.86% | 97.17% | 95.01% | 96.55% | 93.86% | 96.18% | 93.38% |
| **CS-Combined** | 96.90% | 94.05% | 96.27% | 93.04% | 95.58% | 92.40% | 94.43% | 89.80% | 93.21% | 88.32% | 93.05% | 87.75% | 94.41% | 88.90% | 93.55% | 87.86% | 92.79% | 87.36% | 97.26% | 95.23% | 96.87% | 94.68% | 96.08% | 93.19% |
| **FA-Combined** | 96.93% | 94.02% | 96.35% | 93.06% | 95.60% | 91.88% | 94.39% | 89.98% | 93.13% | 88.11% | 93.06% | 87.69% | 94.40% | 89.23% | 93.56% | 87.26% | 92.79% | 87.21% | 97.24% | 95.08% | 96.66% | 93.96% | 96.12% | 92.70% |
| **MODA-Combined** | 97.04% | 94.39% | 96.52% | 93.56% | 96.06% | 92.76% | 94.54% | 90.09% | 93.54% | 88.29% | 93.74% | 88.40% | 94.48% | 89.38% | 93.63% | 87.89% | 92.94% | 87.39% | 97.28% | 95.30% | 97.04% | 94.90% | 96.27% | 93.25% |

**TABLE 11. Grey relational analysis and directionality results.**

| Model | Grey relational analysis | | | | | | | | | | | | Directionality | | | | | | | | | | | |
|---|---|---|---|---|---|---|---|---|---|---|---|---|---|---|---|---|---|---|---|---|---|---|---|---|
| | Spring | | | Summer | | | Autumn | | | Winter | | | Spring | | | Summer | | | Autumn | | | Winter | | |
| | 1-step | 2-step | 3-step | 1-step | 2-step | 3-step | 1-step | 2-step | 3-step | 1-step | 2-step | 3-step | 1-step | 2-step | 3-step | 1-step | 2-step | 3-step | 1-step | 2-step | 3-step | 1-step | 2-step | 3-step |
| **Combined** | **0.8727** | **0.8453** | **0.8842** | **0.847** | **0.8363** | **0.8477** | **0.8417** | **0.8396** | **0.8292** | **0.8717** | **0.8995** | **0.8945** | **0.9301** | **0.9301** | **0.8741** | **0.9021** | **0.8392** | **0.8741** | **0.9231** | **0.8881** | **0.8392** | **0.8951** | **0.8881** | **0.7692** |
| **VMD-ARIMA** | 0.7846 | 0.8142 | 0.8692 | 0.763 | 0.7782 | 0.8002 | 0.7895 | 0.8041 | 0.8222 | 0.8354 | 0.8794 | 0.8778 | 0.8322 | 0.8601 | 0.8462 | 0.7762 | 0.8112 | 0.8112 | 0.8252 | 0.8322 | 0.8462 | 0.7972 | 0.7483 | 0.7343 |
| **VMD-BP** | 0.8266 | 0.837 | 0.829 | 0.8313 | 0.8051 | 0.7439 | 0.8277 | 0.8215 | 0.7852 | 0.8571 | 0.8666 | 0.8263 | 0.8951 | 0.9301 | 0.6853 | 0.9091 | 0.8112 | 0.6503 | 0.9021 | 0.8462 | 0.7133 | 0.8811 | 0.8182 | 0.5664 |
| **VMD-ELM** | 0.8268 | 0.8357 | 0.8209 | 0.8308 | 0.8012 | 0.7419 | 0.8278 | 0.8216 | 0.788 | 0.8506 | 0.8621 | 0.831 | 0.8951 | 0.9301 | 0.6923 | 0.9091 | 0.8112 | 0.6573 | 0.9091 | 0.8322 | 0.7063 | 0.9091 | 0.7762 | 0.5524 |
| **VMD-ENN** | 0.8092 | 0.7369 | 0.775 | 0.8245 | 0.7309 | 0.6781 | 0.7996 | 0.7703 | 0.7646 | 0.8318 | 0.8163 | 0.7848 | 0.8811 | 0.6294 | 0.5315 | 0.8741 | 0.6364 | 0.5664 | 0.8531 | 0.7133 | 0.6713 | 0.8252 | 0.5944 | 0.5594 |
| **ARIMA** | 0.7144 | 0.7355 | 0.8089 | 0.7116 | 0.7281 | 0.7568 | 0.7224 | 0.7537 | 0.7706 | 0.7312 | 0.8203 | 0.8337 | 0.5734 | 0.5594 | 0.5385 | 0.4825 | 0.5664 | 0.5944 | 0.4126 | 0.6014 | 0.6014 | 0.3706 | 0.5874 | 0.5385 |
| **BP** | 0.7127 | 0.6738 | 0.7364 | 0.7232 | 0.644 | 0.6358 | 0.7434 | 0.709 | 0.7262 | 0.763 | 0.7997 | 0.7788 | 0.5594 | 0.5664 | 0.5524 | 0.6154 | 0.5175 | 0.5804 | 0.5664 | 0.6154 | 0.6783 | 0.5385 | 0.5524 | 0.5455 |
| **ELM** | 0.716 | 0.6824 | 0.7486 | 0.7258 | 0.6466 | 0.6349 | 0.7442 | 0.7086 | 0.7259 | 0.7746 | 0.7978 | 0.7808 | 0.5874 | 0.5664 | 0.5594 | 0.6503 | 0.5385 | 0.5455 | 0.5664 | 0.5944 | 0.6923 | 0.5385 | 0.5664 | 0.5524 |
| **ENN** | 0.7229 | 0.6835 | 0.7275 | 0.7297 | 0.6453 | 0.6355 | 0.7432 | 0.7105 | 0.7228 | 0.7653 | 0.8004 | 0.7733 | 0.6224 | 0.5315 | 0.5315 | 0.6224 | 0.5245 | 0.5734 | 0.5874 | 0.6154 | 0.6713 | 0.5524 | 0.5245 | 0.5594 |
| **EMD-Combined** | 0.8087 | 0.82 | 0.8559 | 0.7838 | 0.7678 | 0.7849 | 0.8016 | 0.8137 | 0.8222 | 0.8403 | 0.8656 | 0.8731 | 0.9021 | 0.8811 | 0.8462 | 0.8182 | 0.7692 | 0.7762 | 0.8531 | 0.8531 | 0.8601 | 0.8182 | 0.8112 | 0.7972 |
| **EEMD-Combined** | 0.8137 | 0.8213 | 0.8661 | 0.7781 | 0.7708 | 0.7877 | 0.7971 | 0.8116 | 0.8182 | 0.8492 | 0.8683 | 0.8755 | 0.8881 | 0.8741 | 0.8112 | 0.8322 | 0.7902 | 0.7692 | 0.8601 | 0.8741 | 0.8601 | 0.8462 | 0.7972 | 0.7692 |
| **CEEMD-Combined** | 0.836 | 0.8396 | 0.8704 | 0.8319 | 0.8214 | 0.8387 | 0.834 | 0.821 | 0.8243 | 0.864 | 0.8748 | 0.8789 | 0.8811 | 0.8601 | 0.8322 | 0.9021 | 0.8462 | 0.8671 | 0.8811 | 0.8741 | 0.8531 | 0.8671 | 0.7902 | 0.7483 |
| **CS-Combined** | 0.8299 | 0.836 | 0.8655 | 0.8322 | 0.8142 | 0.8256 | 0.8306 | 0.8226 | 0.8208 | 0.8676 | 0.8832 | 0.8752 | 0.9091 | 0.8881 | 0.8601 | 0.9021 | 0.8322 | 0.8182 | 0.8951 | 0.8671 | 0.8112 | 0.8462 | 0.8322 | 0.7343 |
| **FA-Combined** | 0.8333 | 0.8345 | 0.8661 | 0.8322 | 0.8085 | 0.8278 | 0.8278 | 0.825 | 0.8206 | 0.8604 | 0.8808 | 0.8763 | 0.9301 | 0.8741 | 0.8182 | 0.9021 | 0.8392 | 0.8182 | 0.9091 | 0.8811 | 0.8112 | 0.9021 | 0.8252 | 0.7552 |
| **MODA-Combined** | 0.8414 | 0.834 | 0.8746 | 0.8332 | 0.8217 | 0.8411 | 0.8348 | 0.8239 | 0.8222 | 0.8639 | 0.8819 | 0.8808 | 0.8951 | 0.8601 | 0.8671 | 0.9091 | 0.8601 | 0.8741 | 0.9021 | 0.8741 | 0.8322 | 0.8811 | 0.8462 | 0.7343 |

Compared with the traditional model and the single denoising model, the DM test results are much higher than the critical value of the Compared with the traditional model and the single denoising model, the DM test results are much higher than the critical value of the 10% significance level. Therefore, in this example, the prediction validity of the proposed model and those of the above two models differ significantly. Comparing the other combined models that are based on various denoising strategies, we can find that the proposed VMD-ISMODA combination model performs the best. The minimum DM test value exceeds the threshold value of the 15% level by 1.47. In comparison with the combined model with various optimization methods, the DM test results fluctuate substantially due to the randomness of the algorithm. However, most of the DM values are greater than the critical value of the 10% level. Hence, the proposed VMD-ISMODA model has high predictive performance.

### B. DISCUSSION OF THE FORECASTING EFFECTIVENESS

In this section, to further evaluate the performance of the proposed VMD-ISMODA model, this study applies the indicator of the effectiveness of the prediction. The larger the indicator value, the better the predictive performance of the model. In the first- and second-order predictions, the VMD-ISMODA model has higher forecasting efficiency than the other methods. **Table 10** presents the detailed result values.

Consider the spring dataset as an example. The results of the proposed model in the first-order prediction process are 97.19%. 96.71%, and 96.42% from one-step forecasting to three-step forecasting and the values of the proposed model in the second-order forecasting process are 94.49%, 93.61%, and 93.22%. The values that are obtained by the comparison models are smaller than those of this model. Similarly, in the datasets for the other three seasons, the obtained results are similar to those of the spring dataset. These results provide sufficient evidence that the developed forecasting system outperforms the other models in prediction.

### C. GREY RELATIONAL ANALYSIS AND FORECASTING DIRECTION RESULTS

To more fully evaluate the predictive performance of the model, we introduce two new evaluation indices for in this section: the grey relational analysis index and the direction of forecasting index (GRA and $D_{accuracy}$). The GRA index describes the degree of correlation between the forecasting values and the ground-truth values. The larger the value of the GRA index is, the higher the degree of correlation between the two sequences will be, and the better the model prediction results will be. The directivity index describes the directivity of the latter data point, which corresponds to the directivity of the trend of the original curve and the prediction curve. The larger the value is, the more consistent the directivity of the prediction sequence, and the more accurately of the prediction performance. The values for GRA and $D_{accuracy}$ are presented in **Table 11**, and the values of the developed combined model are identified by bold font in the table. Compared with other prediction models, our proposed VMD-ISMODA combination prediction system has realized excellent prediction performance; hence, the model that is proposed in this study shows a strong advantage compared with other prediction methods.

### D. FORECASTING STABILITY

The accuracy and stability of prediction are highly important indices. The evaluation of forecasting performance cannot rely only on the accuracy, as the stability is indispensable. The innovative combined prediction system that is introduced in this paper was developed based on an improved weight determination method, namely, ISMODA, which aims at increasing the accuracy and stability of model prediction. To more effectively evaluate the prediction performance of the model, we further evaluate the stability of the forecasting values. The stability of the forecasting results is necessary for measuring the prediction performance. In many studies, the variance of the predicted results can often be used to measure the stability of the prediction. Nevertheless, it is unscientific to use the variance of the predicted results to measure the magnitude of the stability because it inadequately reflects the stability of the predicted sequence. Hence, in this section,

**TABLE 12.** Forecasting stability results.

| Model | Spring | | | Summer | | | Autumn | | | Winter | | |
|---|---|---|---|---|---|---|---|---|---|---|---|---|
| | 1-step | 2-step | 3-step | 1-step | 2-step | 3-step | 1-step | 2-step | 3-step | 1-step | 2-step | 3-step |
| **Combined** | **0.3911** | **0.4356** | **0.4889** | **0.2315** | **0.2536** | **0.2536** | **0.2536** | **0.2488** | **0.2691** | **0.2691** | **0.2098** | **0.2674** |
| VMD-ARIMA | 0.5582 | 0.5219 | 0.5430 | 0.3507 | 0.3403 | 0.3403 | 0.3403 | 0.2966 | 0.2933 | 0.2933 | 0.2785 | 0.3056 |
| VMD-BP | 0.4261 | 0.4728 | 0.7566 | 0.2361 | 0.2883 | 0.2883 | 0.2883 | 0.2659 | 0.3874 | 0.3874 | 0.2781 | 0.4567 |
| VMD-ELM | 0.4218 | 0.4727 | 0.7893 | 0.2372 | 0.2970 | 0.2970 | 0.2970 | 0.2656 | 0.3818 | 0.3818 | 0.2893 | 0.4515 |
| VMD-ENN | 0.4779 | 0.8527 | 1.1162 | 0.2506 | 0.4490 | 0.4490 | 0.4490 | 0.3907 | 0.4371 | 0.4371 | 0.4580 | 0.6300 |
| ARIMA | 0.8348 | 0.8418 | 0.8506 | 0.5137 | 0.4930 | 0.4930 | 0.4930 | 0.4363 | 0.4400 | 0.4400 | 0.4342 | 0.4357 |
| BP | 0.8614 | 1.1214 | 1.3482 | 0.4868 | 0.6793 | 0.6793 | 0.6793 | 0.5617 | 0.5662 | 0.5662 | 0.5621 | 0.6696 |
| ELM | 0.8199 | 1.0893 | 1.2985 | 0.4794 | 0.6766 | 0.6766 | 0.6766 | 0.5596 | 0.5622 | 0.5622 | 0.5695 | 0.6676 |
| ENN | 0.8070 | 1.0893 | 1.4018 | 0.4833 | 0.6770 | 0.6770 | 0.6770 | 0.5626 | 0.5697 | 0.5697 | 0.5661 | 0.6856 |
| EMD-Combined | 0.4363 | 0.4906 | 0.6030 | 0.3054 | 0.3496 | 0.3496 | 0.3496 | 0.2807 | 0.3010 | 0.3010 | 0.2730 | 0.2936 |
| EEMD-Combined | 0.4409 | 0.4862 | 0.5523 | 0.3074 | 0.3369 | 0.3369 | 0.3369 | 0.2751 | 0.2928 | 0.2928 | 0.2788 | 0.3002 |
| CEEMD-Combined | 0.4336 | 0.4534 | 0.5630 | 0.2325 | 0.2548 | 0.2548 | 0.2548 | 0.2606 | 0.2802 | 0.2802 | 0.2684 | 0.2726 |
| CS-Combined | 0.4763 | 0.4809 | 0.5599 | 0.2372 | 0.2776 | 0.2776 | 0.2776 | 0.2576 | 0.2845 | 0.2845 | 0.2342 | 0.2840 |
| FA-Combined | 0.4117 | 0.4780 | 0.5535 | 0.2372 | 0.2794 | 0.2794 | 0.2794 | 0.2589 | 0.2943 | 0.2943 | 0.2574 | 0.2963 |
| MODA-Combined | 0.3979 | 0.3967 | 0.5215 | 0.2315 | 0.2560 | 0.2560 | 0.2560 | 0.2538 | 0.2912 | 0.2912 | 0.2215 | 0.2726 |

**TABLE 13.** Results of the sensitivity analysis.

| Dataset | NO. | MAPE (%) | | | MAE | | | RMSE | | | SSE | | |
|---|---|---|---|---|---|---|---|---|---|---|---|---|---|
| | | 1-step | 2-step | 3-step | 1-step | 2-step | 3-step | 1-step | 2-step | 3-step | 1-step | 2-step | 3-step |
| Spring | 10 | 3.03 | 3.56 | 3.74 | 0.3040 | 0.3464 | 0.3647 | 0.4318 | 0.4521 | 0.4774 | 26.8536 | 29.4316 | 32.8137 |
| | 20 | 2.93 | 3.37 | 3.70 | 0.2999 | 0.3251 | 0.3687 | 0.4131 | 0.4363 | 0.4927 | 24.5781 | 27.4053 | 34.9514 |
| | **30** | **2.81** | **3.29** | **3.58** | **0.2814** | **0.3144** | **0.3568** | **0.3935** | **0.4373** | **0.4913** | **22.2917** | **27.5359** | **34.7631** |
| | 40 | 2.97 | 3.41 | 3.64 | 0.3054 | 0.3330 | 0.3673 | 0.4265 | 0.4430 | 0.5008 | 26.1942 | 28.2549 | 36.1145 |
| Summer | 10 | 5.63 | 6.69 | 6.21 | 0.1807 | 0.2091 | 0.2091 | 0.2348 | 0.2650 | 0.2761 | 7.9399 | 10.1132 | 10.9795 |
| | 20 | 5.51 | 6.45 | 6.13 | 0.1778 | 0.2095 | 0.2073 | 0.2315 | 0.2624 | 0.2739 | 7.7159 | 9.9135 | 10.7996 |
| | **30** | **5.02** | **6.08** | **5.85** | **0.1632** | **0.2002** | **0.1992** | **0.2181** | **0.2532** | **0.2668** | **6.8523** | **9.2344** | **10.2473** |
| | 40 | 5.52 | 6.69 | 6.05 | 0.1811 | 0.2091 | 0.2082 | 0.2316 | 0.2650 | 0.2788 | 7.7225 | 10.1132 | 11.1962 |
| Autumn | 10 | 5.46 | 6.63 | 6.94 | 0.1725 | 0.2072 | 0.2204 | 0.2192 | 0.2633 | 0.2761 | 6.9175 | 9.9833 | 10.9794 |
| | 20 | 5.25 | 6.22 | 6.78 | 0.1687 | 0.1947 | 0.2148 | 0.2151 | 0.2510 | 0.2697 | 6.6639 | 9.0748 | 10.4713 |
| | **30** | **5.05** | **6.15** | **6.74** | **0.1632** | **0.1945** | **0.2153** | **0.2127** | **0.2482** | **0.2682** | **6.5172** | **8.869** | **10.3548** |
| | 40 | 5.29 | 6.34 | 6.94 | 0.1697 | 0.2023 | 0.2204 | 0.2162 | 0.2524 | 0.2761 | 6.7280 | 9.1711 | 10.9794 |
| Winter | 10 | 2.91 | 2.95 | 3.92 | 0.1745 | 0.1766 | 0.2378 | 0.2260 | 0.2236 | 0.3046 | 7.3540 | 7.2007 | 13.3611 |
| | 20 | 2.81 | 2.87 | 3.66 | 0.1636 | 0.1719 | 0.2184 | 0.2030 | 0.2216 | 0.2771 | 5.9367 | 7.0745 | 11.0588 |
| | **30** | **2.46** | **2.6** | **3.4** | **0.1497** | **0.1599** | **0.2087** | **0.1944** | **0.2094** | **0.2668** | **5.4428** | **6.3131** | **10.2535** |
| | 40 | 2.68 | 2.87 | 3.75 | 0.1569 | 0.1731 | 0.2246 | 0.1994 | 0.2227 | 0.2816 | 5.7249 | 7.1404 | 11.4183 |

the standard deviation of the prediction error is used to evaluate the magnitude of the stability index. The improved stability index combines the sequence characteristics of both the predicted curve and the ground-truth curve to more effectively demonstrate the predictive performance. The obtained indicator values are presented in **Table 12**. In the comparison with the other considered models, the proposed combined model realizes the highest stability; hence, it realizes satisfactory prediction performance.

### *E. SENSITIVITY ANALYSIS*

In the proposed combined prediction system, the optimization module plays a key role, and the VMD-ISMODA optimization algorithm has a substantial influence on improving the prediction accuracy. Therefore, the parameter setting problem in the optimization algorithm merits discussion. During the optimization of the algorithm, a key parameter, namely, the number of search agents, affects the performance of the algorithm and affects the prediction performance of the prediction model. In this section, we conduct a sensitivity analysis on the number of search agents. We design a variety of agent number running models, and the prediction results are presented in **Table 13**. According to the prediction results, the forecasting accuracy changes with the number of agents. Too many agents can lead to inaccurate predictions and can increase the complexity of the algorithm, whereas if the number of agents is too small, the optimal weighting factor cannot be obtained, thereby leading to inaccurate predictions. The total number of agents is determined via an optimization process for the algorithm. According to the results in **Table 13**, there is a turning point in the number of agents, which can be used as the optimal parameter of the algorithm. Based on the above discussion, we set the number of search agents to 30, which is the result of several trials that optimized the performance of the model.

## VII. CONCLUSION

The role of wind energy in the field of low-carbon energy cannot be ignored. Reliable and accurate forecasting has important economic and security implications for the operation of wind farms. Nevertheless, forecasting remains a difficult problem that must be solved urgently due to the complexity and nonlinear characteristics of wind speed datasets. In this study, a combined wind energy forecasting system is proposed, which is based on variational mode decomposition technology and the immune selection multi-objective dragonfly optimization algorithm, and stable and accurate forecasting results are obtained. The wind speed data of four seasons in China's wind farms are used to evaluate the results, which prove the predictive accuracy and performance of the combined forecasting system that is proposed in this study. As one of the countries with the largest installed wind power capacity in the world, the wind speed data of China is representative and experimental. The experimental results demonstrate that the combined forecasting system that is proposed in this paper has the following advantages: (a) after adopting the improved multi-objective optimization algorithm, it not only improves the accuracy of prediction but also ensures the stability of the prediction results; and (b) the experimental module and evaluation module show that the model realizes satisfactory predictive performance. In the end, the above analysis shows that the proposed combined model forecasting system has extremely high predictive power and, hence, can be used as an effective tool for wind energy forecasting. The combined wind speed forecasting system proposed in this paper can effectively realize the utilization of wind energy resources and play a significant role in the power dispatching and management of wind farms. The proposed forecasting system can be used for wind speed forecasting in other regions, but none of the models is perfect. When considering data in different regions, we need to consider appropriate adjustments to the forecasting system.

## APPENDIX

See Tables 14 and 15.

**TABLE 14.** The general settings for model parameters.

| Parameter setting of VMD algorithm | | |
|---|---|---|
| Parameters to describe | Parameter | Specifications |
| moderate bandwidth constraint | *alpha* | 2000 |
| noise-tolerance (no strict fidelity enforcement) | *tau* | 0 |
| the number of modes to be recovered | *K* | 10 |
| no DC part imposed | *DC* | 0 |
| initialize omegas uniformly | *init* | 1 |
| tolerance of convergence criterion | *tol* | 1.00e-07 |

| Parameter setting of BP, ENN, ELM | | | |
|---|---|---|---|
| Parameters to describe | BP | ENN | ELM |
| Number layers | 3 | 3 | 3 |
| Neurons (layer 1) – inputs | 5 | 5 | 5 |
| Neurons (layer 2) – hidden | 10 | 25 | 20 |
| Neurons (layer 3) – output | 1-3 | 1-3 | 1-3 |
| Activation function | Tansig | Sigmoid | sigmod |
| epoch | 1000 | 1000 | - |

| Parameter setting of IS-MODA | | |
|---|---|---|
| Parameters to describe | Parameter | Specifications |
| Iteration Number | - | 500 |
| Archive Size | - | 100 |
| Dragonfly Number | - | 30 |
| Number of optimization parameters | - | 4 |
| Decision parameters of IS | *DS* | 8 |
| Probability of immune replace | *replaceP* | 0.5 |
| Smallest distance between individuals | *minD* | $1e-10$ |

**TABLE 15.** The running time of the models (s).

| Model | Spring | Summer | Autumn | Winter | Mean |
|---|---|---|---|---|---|
| | Mean of 1 to 3 steps | | | | |
| **Combined** | **86.8154** | **83.8690** | **89.5728** | **86.1775** | **86.6087** |
| **VMD-ARIMA** | 23.5444 | 21.2459 | 22.4596 | 21.2126 | 22.1156 |
| **VMD-BP** | 15.2484 | 15.5050 | 15.0898 | 14.6723 | 15.1289 |
| **VMD-ELM** | 13.8742 | 13.1413 | 13.6758 | 13.6647 | 13.5890 |
| **VMD-ENN** | 15.8212 | 16.1207 | 15.5709 | 15.4841 | 15.7492 |
| **ARIMA** | 10.9200 | 9.3529 | 10.0274 | 10.8568 | 10.2893 |
| **BP** | 3.6240 | 3.6119 | 3.6056 | 3.2965 | 3.5345 |
| **ELM** | 2.2498 | 2.2482 | 2.2436 | 2.2889 | 2.2576 |
| **ENN** | 4.1968 | 4.2276 | 4.1387 | 4.1083 | 4.1679 |
| **EMD-Combined** | 48.2430 | 46.1811 | 52.5044 | 51.2255 | 49.5385 |
| **EEMD-Combined** | 152.8754 | 156.6531 | 160.3336 | 161.1123 | 157.7436 |
| **CEEMD-Combined** | 71.8522 | 64.9471 | 70.8268 | 72.4367 | 70.0157 |
| **CS-Combined** | 78.9939 | 76.6378 | 77.2895 | 75.7697 | 77.1727 |
| **FA-Combined** | 76.7824 | 74.2524 | 75.0016 | 73.4173 | 74.8634 |
| **MODA-Combined** | 79.3569 | 83.7172 | 77.2649 | 83.0329 | 80.8430 |

## REFERENCES


[1] A. Tascikaraoglu and M. Uzunoglu, "A review of combined approaches for prediction of short-term wind speed and power," *Renew. Sustain. Energy Rev.*, vol. 34, pp. 243–254, Jun. 2014.

[2] H. Yang, Z. Jiang, and H. Lu, "A hybridwind speed forecasting system based on a 'decomposition and ensemble' strategy and fuzzy time series," *Energies*, vol. 10, no. 9, p. 1422, 2017.

[3] C. Wu, J. Wang, X. Chen, P. Du, and W. Yang, "A novel hybrid system based on multi-objective optimization for wind speed forecasting," *Renew. Energy*, vol. 146, pp. 149–165, Feb. 2020.

[4] C. Rica. Global Wind Energy Council. Brussels, Belgium. (2017). *Global Wind Statistics*. Accessed: 2018. [Online]. Available: http://www.gwec.net/wpcontent/uploads/vip/GWEC_PRstats2017_EN_WEB.pdf

[5] X. Niu and J. Wang, "A combined model based on data preprocessing strategy and multi-objective optimization algorithm for short-term wind speed forecasting," *Appl. Energy*, vol. 241, pp. 519–539, May 2019.

[6] P. Jiang and Z. Liu, "Variable weights combined model based on multi-objective optimization for short-term wind speed forecasting," *Appl. Soft Comput.*, vol. 82, Jun. 2019, Art. no. 105587.

[7] P. Du, J. Z. Wang, W. D. Yang, and T. Niu, "A novel hybrid model for short-term wind power forecasting," *Appl. Soft. Comput.*, vol. 80, pp. 93–106, Jul. 2019.

[8] Y. Hao and C. Tian, "A novel two-stage forecasting model based on error factor and ensemble method for multi-step wind power forecasting," *Appl. Energy*, vol. 238, pp. 368–383, Mar. 2019.

[9] L. Landberg, "Short-term prediction of local wind conditions," *J. Eng. Ind. Aerodynamics*, vol. 89, nos. 3–4, pp. 235–245, 2001.

[10] M. Negnevitsky, P. Johnson, and S. Santoso, "Short term wind power forecasting using hybrid intelligent systems," in *Proc. IEEE Power Eng. Soc. Gen. Meeting*, Jun. 2007, pp. 1–4.

[11] C. Tian, Y. Hao, and J. Hu, "A novel wind speed forecasting system based on hybrid data preprocessing and multi-objective optimization," *Appl. Energy*, vol. 231, pp. 301–319, Dec. 2018.

[12] S. S. Soman, H. Zareipour, O. Malik, and P. Mandal, "A review of wind power and wind speed forecasting methods with different time horizons," in *Proc. North Amer. Power Symp.*, Sep. 2010, pp. 1–8.

[13] J. Wang, P. Du, H. Lu, W. Yang, and T. Niu, "An improved grey model optimized by multi-objective ant lion optimization algorithm for annual electricity consumption forecasting," *Appl. Soft Comput.*, vol. 72, pp. 321–337, Nov. 2018.

[14] H. Liu, H.-Q. Tian, D.-F. Pan, and Y.-F. Li, "Forecasting models for wind speed using wavelet, wavelet packet, time series and artificial neural networks," *Appl. Energy*, vol. 107, pp. 191–208, Jul. 2013.

[15] L. Yu, A. Han, L. Wang, X. Jia, and Z. Zhang, "Short-Term load forecasting model for metro power supply system based on echo state neural network," in *Proc. 7th IEEE Int. Conf. Softw. Eng. Service Sci. (ICSESS)*, Aug. 2016, pp. 906–909.

[16] R. Blonbou, "Very short-term wind power forecasting with neural networks and adaptive Bayesian learning," *Renew. Energy*, vol. 36, no. 3, pp. 1118–1124, 2011.

[17] C. H. Cheng and L. Y. Wei, "A novel time-series model based on empirical mode decomposition for forecasting TAIEX," *Econ. Model.*, vol. 36, pp. 136–141, Jan. 2014.

[18] H. Li, J. Wang, H. Lu, and Z. Guo, "Research and application of a combined model based on variable weight for short term wind speed forecasting," *Renew. Energy*, vol. 116, pp. 669–684, Feb. 2018.

[19] Y. Hao and C. Tian, "The study and application of a novel hybrid system for air quality early-warning," *Appl. Soft Comput.*, vol. 74, pp. 729–746, Jan. 2019.

[20] B. Kordanuli, L. Barjaktarović, L. Jeremić, and M. Alizamir, "Appraisal of artificial neural network for forecasting of economic parameters," *Phys. A, Stat. Mech. Appl.*, vol. 465, pp. 515–519, Jan. 2017.

[21] J. Wang, T. Niu, H. Lu, W. Yang, and P. Du, "A novel framework of reservoir computing for deterministic and probabilistic wind power forecasting," *IEEE Trans. Sustain. Energy*, to be published.

[22] X. Zhang, J. Wang, and Y. Gao, "A hybrid short-term electricity price forecasting framework: Cuckoo search-based feature selection with singular spectrum analysis and SVM," *Energy Econ.*, vol. 81, pp. 899–913, Jun. 2019.

[23] X. Ma, Y. Jin, and Q. Dong, "A generalized dynamic fuzzy neural network based on singular spectrum analysis optimized by brain storm optimization for short-term wind speed forecasting," *Appl. Soft. Comput.*, vol. 54, pp. 296–312, May 2017.

[24] G. Li and J. Shi, "On comparing three artificial neural networks for wind speed forecasting," *Appl. Energy*, vol. 87, no. 7, pp. 2313–2320, 2010.

[25] J. Wang, C. Wu, and T. Niu, "A novel system for wind speed forecasting based on multi-objective optimization and echo state network," *Sustainability*, vol. 11, no. 2, pp. 1–34, 2019.

[26] T. Niu, J. Wang, H. Lu, and P. Du, "Uncertainty modeling for chaotic time series based on optimal multi-input multi-output architecture: Application to offshore wind speed," *Energy Convers. Manage.*, vol. 156, pp. 597–617, Jan. 2018.

[27] H. Wang, H. Yi, J. Peng, G. Wang, Y. Liu, H. Jiang, and W. Liu, "Deterministic and probabilistic forecasting of photovoltaic power based on deep convolutional neural network," *Energy Convers. Manage.*, vol. 153, pp. 409–422, Dec. 2017.

[28] Y.-L. Hu and L. Chen, "A nonlinear hybrid wind speed forecasting model using LSTM network, hysteretic ELM and differential evolution algorithm," *Energy Convers. Manage.*, vol. 173, pp. 123–142, Oct. 2018.
[29] H. Li, J. Wang, R. Li, and H. Lu, "Novel analysis-forecast system based on multi-objective optimization for air quality index," *J. Cleaner Prod.*, vol. 208, pp. 1365–1383, Jan. 2019.
[30] Z.-H. Guo, J. Wu, H.-Y. Lu, and J.-Z. Wang, "A case study on a hybrid wind speed forecasting method using BP neural network," *Knowl.-Based Syst.*, vol. 24, no. 7, pp. 1048–1056, 2011.
[31] C. Tian and Y. Hao, "A novel nonlinear combined forecasting system for short-term load forecasting," *Energies*, vol. 11, no. 14, p. 712, 2018.
[32] X. Ma, Y. S. Hu, and Z. B. Liu, "A novel kernel regularized nonhomogeneous grey model and its applications," *Commun. Nonlinear Sci. Numer. Simul.*, vol. 48, pp. 51–62, Jul. 2017.
[33] J. Heng, C. Wang, X. Zhao, and J. Wang, "A hybrid forecasting model based on empirical mode decomposition and the cuckoo search algorithm: A case study for power load," *Math. Problems Eng.*, vol. 2016, pp. 1–28, Dec. 2016.
[34] S. Wang, N. Zhang, L. Wu, and Y. Wang, "Wind speed forecasting based on the hybrid ensemble empirical mode decomposition and GA-BP neural network method," *Renew. Energy*, vol. 94, pp. 629–636, Aug. 2016.
[35] Q. Zhou, C. Wang, and G. Zhang, "Hybrid forecasting system based on an optimal model selection strategy for different wind speed forecasting problems," *Appl. Energy*, vol. 250, pp. 1559–1580, Sep. 2019.
[36] K. M. Nor, M. Shaaban, and H. Abdul Rahman, "Feasibility assessment of wind energy resources in Malaysia based on NWP models," *Renew. Energy*, vol. 62, pp. 147–154, Feb. 2014.
[37] C. Gallego, P. Pinson, H. Madsen, A. Costa, and A. Cuerva, "Influence of local wind speed and direction on wind power dynamics—Application to offshore very short-term forecasting," *Appl. Energy*, vol. 88, no. 11, pp. 4087–4096, 2011.
[38] L. Lazić, G. Pejanović, and M. Živković, "Wind forecasts for wind power generation using the Eta model," *Renew. Energy*, vol. 35, no. 6, pp. 1236–1243, 2010.
[39] O. A. Maatallah, A. Achuthan, K. Janoyan, and P. Marzocca, "Recursive wind speed forecasting based on Hammerstein auto-regressive model," *Appl. Energy*, vol. 145, pp. 191–197, May 2015.
[40] V. Radziukynas and A. Klementavicius, "Short-term wind speed forecasting with ARIMA model," in *Proc. 55th Int. Sci. Conf. Power Elect. Eng. Riga Tech. Univ.*, 2014, pp. 145–149.
[41] R. G. Kavasseri and K. Seetharaman, "Day-ahead wind speed forecasting using f-ARIMA models," *Renew. Energy*, vol. 34, no. 5, pp. 1388–1393, 2009.
[42] E. Cadenas and W. Rivera, "Short term wind speed forecasting in La Venta, Oaxaca, México, using artificial neural networks," *Renew. Energy*, vol. 34, no. 1, pp. 274–278, 2009.
[43] L. Zjavka, "Wind speed forecast correction models using polynomial neural networks," *Renew. Energy*, vol. 83, pp. 998–1006, Nov. 2015.
[44] J. Zhou, J. Shi, and G. Li, "Fine tuning support vector machines for short-term wind speed forecasting," *Energy Convers. Manage.*, vol. 52, no. 4, pp. 1990–1998, 2011.
[45] P. Du, J. Wang, W. Yang, and T. Niu, "Container throughput forecasting using a novel hybrid learning method with error correction strategy," *Knowl.-Based Syst.*, vol. 182, Oct. 2019, Art. no. 104853.
[46] Y. Zhang, J. Wang, and H. Lu, "Research and application of a novel combined model based on multiobjective optimization for multistep-ahead electric load forecasting," *Energies*, vol. 12, no. 10, p. 1931, 2019.
[47] H. Wang, Z. Lei, X. Zhang, B. Zhou, and J. Peng, "A review of deep learning for renewable energy forecasting," *Energy Convers. Manag.*, vol. 198, 2019, Art. no. 111799.
[48] G. W. Chang and H. J. Lu, "Integrating grey data preprocessor and deep belief network for day-ahead PV power output forecast," *EEE Trans. Sustain. Energy*, to be published.
[49] H.-F. Yang, T. S. Dillon, and Y.-P. P. Chen, "Optimized structure of the traffic flow forecasting model with a deep learning approach," *IEEE Trans. Neural Netw. Learn. Syst.*, vol. 28, no. 10, pp. 2371–2381, Oct. 2017.
[50] U. Maji, M. Mitra, and S. Pal, "Detection and characterisation of QRS complex in VMD domain," in *Proc. Michael Faraday IET Int. Summit*, Sep. 2015, pp. 586–590.
[51] K. Dragomiretskiy and D. Zosso, "Variational mode decomposition," *IEEE Trans. Signal Process.*, vol. 62, no. 3, pp. 531–544, Feb. 2014.
[52] S. Mirjalili, "Dragonfly algorithm: A new meta-heuristic optimization technique for solving single-objective, discrete, and multi-objective problems," *Neural Comput. Appl.*, vol. 27, no. 4, pp. 1053–1073, 2016.
[53] Y. Qi, X. L. Ma, F. Liu, L. Jiao, J. Sun, and J. Wu, "MOEA/D with adaptive weight adjustment," *Evol. Comput.*, vol. 22, no. 2, pp. 231–264, 2014.
[54] Z. Yang, Y. Ding, K. Hao, and X. Cai, "An adaptive immune algorithm for service-oriented agricultural Internet of Things," *Neurocomputing*, vol. 344, pp. 3–12, Jun. 2019.
[55] K. Honda and D. R. Littman, "The microbiota in adaptive immune homeostasis and disease," *Nature*, vol. 535, no. 7610, pp. 75–84, 2016.
[56] F. Liu, F. Sun, W. Liu, T. Wang, H. Wang, and X. Wang, "On wind speed pattern and energy potential in China," *Appl. Energy*, vol. 236, pp. 867–876, Feb. 2020.
[57] S. Zhang, Y. Liu, J. Wang, and C. Wang, "Research on combined model based on multi–objective optimization and application in wind speed forecast," *Appl. Sci.*, vol. 9, no. 3, p. 423, 2019.
[58] P. Jiang, H. Yang, and X. Ma, "Coal production and consumption analysis, and forecasting of related carbon emission: Evidence from China," *Carbon Manage.*, vol. 10, no. 2, pp. 189–208, 2019.
[59] R. Li and Y. Jin, "A wind speed interval prediction system based on multi-objective optimization for machine learning method," *Appl. Energy*, vol. 228, pp. 2207–2220, Oct. 2018.
[60] P. Jiang, R. Li, and H. Li, "Multi-objective algorithm for the design of prediction intervals for wind power forecasting model," *Appl. Math. Model.*, vol. 67, pp. 101–122, Mar. 2019.
[61] Y. Hao, C. Tian, and C. Wu, "Modelling of carbon price in two real carbon trading markets," *J. Clean. Prod.*, vol. 244, Jan. 2019, Art. no. 118556.


**HE BO** received the Ph.D. degree from the Tianjin University of Finance and Economics, in 2011. She currently holds a postdoctoral position at the School of Economics, Dongbei University of Finance and Economics. She has published some refereed journal articles. Her research interests include computational intelligence, macroeconomic analysis, and wind speed forecasting.

**XINSONG NIU** received the B.S. degree from Shandong Agricultural University, in 2013. He is currently pursuing the master's degree with the Dongbei University of Finance and Economics. His research interests include artificial intelligence, optimization algorithms, machine learning, and time series forecasting.

**JIANZHOU WANG** received the B.S. degree from Northwest Normal University, in 1988, and the M.Sc. and Ph.D. degrees from Lanzhou University, in 1998 and 2004, respectively. He is currently a Professor with the School of Statistics, Dongbei University of Finance and Economics. He has published over 150 refereed journal articles. His research interests are in the areas of wind energy forecasting, data mining, machine learning, statistics learning, and forecast theory.